

Optimization of Hybrid Composite Laminates with Various Materials using the GA/GPSA Hybrid Algorithm for Maximum Dimensional Stability

Hacer GEÇMEZ¹, Hamza Arda DEVECİ^{2*}

¹ Department of Mechanical Engineering, Graduate School of Natural and Applied Sciences, Erzincan Binali Yıldırım University, Yalnızbağ Yerleşkesi, 24002, Erzincan, Turkey.

² Department of Mechanical Engineering, Faculty of Engineering and Architecture, Erzincan Binali Yıldırım University, Yalnızbağ Yerleşkesi, 24002, Erzincan, Turkey. (ORCID: [0000-0003-3255-1504](https://orcid.org/0000-0003-3255-1504)) (ORCID: [0000-0001-9926-8768](https://orcid.org/0000-0001-9926-8768))



Keywords: Dimensional stability, Optimization, Hybrid composite laminates, GA/GPSA hybrid algorithm.

Abstract

In this study, it is aimed at obtaining the highest dimensional stability against temperature changes in fiber-reinforced hybrid composite laminates considering eight different composite materials: Aramid/Epoxy, AS4/Epoxy, Boron/Epoxy, E-Glass/Epoxy, IM6/Epoxy, GY70/Epoxy, Kevlar49/Epoxy, and Spectra/Epoxy. The study focuses on finding the optimum continuous and traditional fiber angle orientations for the hybrid composite plates that would provide the lowest coefficients of thermal expansion. For this purpose, two different laminate sequences were investigated, each including two materials. A hybrid algorithm combining a genetic algorithm and a generalized pattern search algorithm was used in the optimization. A great number of hybrid design problems were solved repeatedly, and their results were compared both within themselves and to the optimum non-hybrid laminate results. Furthermore, the thermal durability of the selected optimum hybrid designs was evaluated using Tsai-Wu failure and Hashin-Rotem criteria. The results reveal that a substantial increase in dimensional stability can be achieved by stacking sequence optimization of hybrid composite laminates with multiple material selections, and this hybrid design approach can offer the desired laminated composite structures for aerospace applications required to withstand extreme temperature changes.

1. Introduction

Fiber-reinforced composites have become indispensable materials in many engineering applications, including on land, at sea, and in the air, as well as providing many advantages over other traditional materials. With the development of technology, the use of these alternative materials has been an important subject in line with the different needs and expectations of industry. In this regard, it can be said that dimensionally stable composite materials are those materials desired to meet the expectations in satellite applications today. Fiber-reinforced composite materials have the best

potential to meet the need for dimensional stability since their tailorability properties give them a chance to obtain very small geometrical changes when exposed to environmental influences such as humidity and temperature.

Dimensional stability is directly related to the material properties, including the coefficient of thermal expansion (CTE) and the coefficient of moisture expansion. Besides, thermal and moisture effects are parameters that should not be disregarded for the dimensional stability of polymer matrix composites and change the mechanical properties of the materials significantly. Unexpected results may emerge during service when these parameters are not

*Corresponding author: hadeveci@erzincan.edu.tr

Received: 03.09.2023, Accepted: 02.01.2024

considered in the design of composite material applications in engineering. For this reason, there is much ongoing research that investigates the thermal and moisture effects on laminated composite structures in the literature. For instance, Lim and Hong [1] used a modified shear delay analysis to examine the effects of the stiffness reduction and thermal expansion coefficient variation caused by transverse cracks in cross-layer laminate composites. The results showed that transverse cracks reduce the effective stiffness and coefficient of thermal expansion of composite laminates; at the same time, the stiffness reduction and change in the laminate thermal expansion coefficient due to transverse cracks were deeply affected by the laminate configuration. Yoon and Ki [2] studied the estimation of the coefficients of thermal expansion to determine the temperature variation of Carbon/Epoxy laminate materials. For this purpose, a computational method is proposed to estimate the variation of the coefficients of thermal expansion of an overall laminate for temperature variation. In the research, elastic properties and coefficients of thermal expansion in the material's main directions were measured in the range from room temperature to curing temperature and characterized as temperature functions. The coefficients of thermal expansion of laminates with different angles were measured and compared with the predicted ones. Experimental results show that changes in the coefficients of thermal expansion of an overall laminate for temperature change can be well estimated using the proposed method. Kim and Crasto [3] considered aerospace structural materials and investigated the changes in coefficients of thermal expansion using two representative materials. It was aimed at accurately determining low CTE values in the study. The results show that the change in coefficients of thermal expansion due to ply cracking in the cross-ply laminates can be quantitatively predicted under thermal cycling and mechanical loadings.

On the other hand, optimum stacking sequence design for dimensionally stable composite structures has been considered in the literature to prevent and minimize the negative effects of thermal and moisture factors. However, there are limited studies on optimum stacking sequence design for dimensionally stable composite structures. As pioneers in this field, Riche and Gaudin [4] studied the effectiveness of optimizing fiber orientation angles to minimize plate bending problems and achieve dimensional stability in composite structures. By optimizing the stacking sequences, the researchers could deliver the desired performance

and reduce the negative effects of production-related issues. Khalil et al. [5] investigated the effect of hygrothermal residual stresses on the optimum design of laminated composite materials, which was analyzed theoretically. In this study, composite materials exposed to different mechanical, thermal, and humidity loads were investigated. The results showed that among the selected materials, E-glass/epoxy and Kevlar/epoxy have greater moisture absorption capacity compared to other materials when designing optimum composite laminates under thermal and moisture loadings. In addition, the optimum material properties based on the thermal expansion coefficient of the selected composite laminates were investigated by Zhu and Sun [6] using an evolution algorithm. As a result of the research, it was determined that the ratio of plane shear modulus to fiber directional modulus of elasticity has a significant effect on the thermal expansion coefficient. Diaconu and Sekine [7] considered the temperature and moisture parameters affecting the composite materials and suggested an optimization problem to provide minimum displacement in terms of transverse characteristics. In the study of Aydin and Artem [8], it was aimed at finding the optimum stacking sequences of symmetric and balanced laminated carbon/epoxy composites with different numbers of layers. Both single-objective and multi-objective optimization approaches were utilized in the design process. The results show that stacking sequences with lower thermal expansion coefficients and higher elastic modulus can be obtained by continuous laminate designs rather than conventional ones.

Besides the optimization for dimensionally stable composites using a single composite material in laminates, this process may include designing the composite material to have more than one fiber or matrix material. In this regard, optimization studies of hybrid composite laminates constituted using numerous composite materials to ensure maximum dimensional stability have been present in the literature. For instance, in the study of Zhang et al. [9], an optimization was conducted to estimate the thermal expansion coefficients and mechanical properties of hybrid composites used in aerospace. As a result of the dimensional stability optimization, both the optimal design of hybrid composites with zero thermal expansion coefficient and the optimum design of hybrid composite plates with minimum thermal expansion coefficient were found. Bressan et al. [10] addressed the issue of hybrid material component optimization and design patterns made of carbon-epoxy laminates with low thermal expansion. The effects of selected hybrid materials on the

behavior of the composite, such as structural and thermo-elastic mismatches, were investigated using evolutionary strategy algorithms. They reported that hybrid composite materials used in satellite equipment are optimal in terms of minimum mass and high resonance.

Hybridization of laminates can also provide improvements for the other objectives of composite materials. For example, Adali and Duffy [11], with a single-purpose approach, optimized the fiber orientation of antisymmetric and angle-ply hybrid layer structures to further increase cost-effectiveness with a natural frequency constraint. Adali and Verijenko [12] presented a study in which natural frequency, frequency separation, and cost factors were discussed for hybrid graphite-glass/epoxy inter-ply hybrid layer structures, and at the end, optimum fiber orientations of the hybrid composites were obtained. Abachizadeh and Tahani [13] proposed a procedure that covers the design and optimization of a graphite-glass/epoxy hybrid composite with a symmetrical inter-ply hybrid layer structure. Both the maximum natural frequency and minimum cost objectives based on the multi-objective optimization approach have been successfully carried out. It was reported that hybridization provides a reasonable reduction in fundamental frequency for a remarkable reduction in material cost. Aydin and Savran [14] aimed to find the number of high-hardness and cheaper laminates that maximize the fundamental frequency and minimize the cost with the multi-objective optimization approach of stacking sequence design and optimization in inter-ply hybrid composite structures. The results show that the proposed optimum graphite-flax/epoxy composite structure outperforms in terms of maximum fundamental frequency and minimum cost.

As seen in the literature, the studies generally consider a limited number of composite materials in the hybridization process and conventional fiber angles in the stacking sequence designs. Furthermore, these studies did not propose a general, comprehensive, and optimum hybrid design

procedure using many different composite materials using a novel hybrid algorithm not utilized in the field. In this respect, in the present study, the optimum stacking sequence designs of 16-layered symmetric hybrid composite laminates considering various materials were investigated to obtain the lowest thermal expansion coefficients. Aramid/Epoxy, AS4/Epoxy, Boron/Epoxy, E-Glass/Epoxy, IM6/Epoxy, GY70/Epoxy, Kevlar49/Epoxy, and Spectra/Epoxy composite materials were used to hybridize the laminates. Numerous optimization problems were constituted considering continuous, discrete fiber angles and two different material sequences in laminates. These optimum design problems were solved by a powerful hybrid algorithm that is a combination of a genetic algorithm and a generalized pattern search algorithm. Afterward, by selecting the best dimensionally stable designs among all the optimum designs, it was checked whether the thermal stresses that will occur under certain positive and negative temperature changes are in the safe zone with two different composite failure theories.

Considering the studies in the literature, it can be said that the effect of hybridization of multiple materials in specific material sequences and optimization of stacking sequences on the dimensional stability of composite laminates was not thoroughly considered. In this regard, this study proposes a reliable optimum hybrid composite design procedure for maximum dimensional stability in applications that require minimum thermal stresses, including a verification study of the optimum design procedure by testing the designs under thermal loading.

In this study, objective functions in the optimization problems concerning dimensionally stable composite laminates were constituted based on classical lamination theory. Figure 1 shows a representative laminated composite plate with global and local coordinates subjected to thermal loading, ΔT .

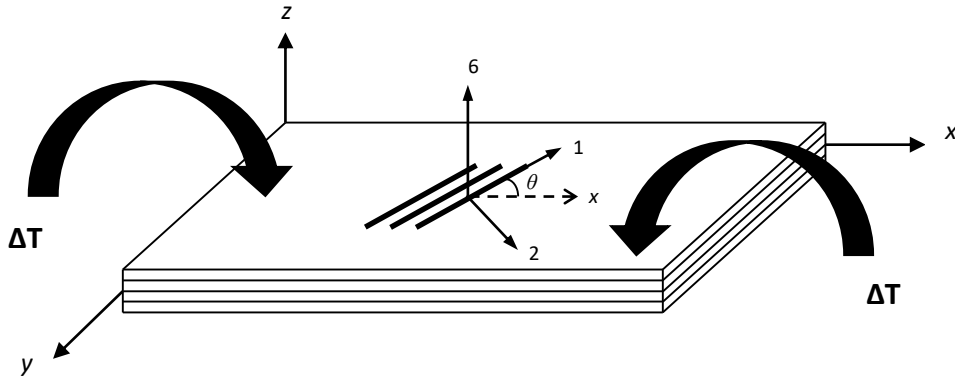


Figure 1. Layered composite plate with global and local coordinates [16]

2. Mechanics of Dimensional Stability

In this study, objective functions in the optimization problems concerning dimensionally stable composite laminates were constituted based on classical lamination theory (CLT) [15]. Figure 1 shows a representative laminated composite plate with global and local coordinates subjected to thermal loading, ΔT .

According to the CLT, the relation between stress and strain of an angled composite layer (k) can be given as follows:

$$\begin{bmatrix} \sigma_x \\ \sigma_y \\ \tau_{xy} \end{bmatrix}_k = \begin{bmatrix} \bar{Q}_{11} & \bar{Q}_{12} & \bar{Q}_{16} \\ \bar{Q}_{12} & \bar{Q}_{22} & \bar{Q}_{26} \\ \bar{Q}_{16} & \bar{Q}_{26} & \bar{Q}_{66} \end{bmatrix}_k \begin{bmatrix} \varepsilon_x \\ \varepsilon_y \\ \gamma_{xy} \end{bmatrix}_k \quad (1)$$

where $[\bar{Q}_{ij}]$ ($i, j = x, y$) is transformed reduced stiffness matrix and $[\varepsilon_{ij}]$ ($i, j = x, y$) indicates mid-plane strains.

In-plane normal resultant forces, N_x, N_y , and shear resultant force, N_{xy} applied on composite plates can be defined as

$$\begin{bmatrix} N_x \\ N_y \\ N_{xy} \end{bmatrix}_k = \begin{bmatrix} A_{11} & A_{12} & A_{16} \\ A_{12} & A_{22} & A_{26} \\ A_{16} & A_{26} & A_{66} \end{bmatrix}_k \begin{bmatrix} \varepsilon_x^0 \\ \varepsilon_y^0 \\ \gamma_{xy}^0 \end{bmatrix} \quad (2)$$

in which $[A]$ corresponds to the extensional stiffness matrix and $[\varepsilon^0]$ is the mid-plane strain matrix of the plate. The elements of $[A]$ matrix are expressed as

$$A_{ij} = \sum_{k=1}^n [\bar{Q}_{ij}]_k (h_k - h_{k-1}) \quad (3)$$

The behavior of laminated composite plates under thermal effects is considered in this study. In this regard, in-plane thermal loads per unit length that occur in a lamina can be expressed as

$$\begin{bmatrix} N_x \\ N_y \\ N_{xy} \end{bmatrix}_k = \Delta T \sum_{k=1}^n \begin{bmatrix} \bar{Q}_{11} & \bar{Q}_{12} & \bar{Q}_{16} \\ \bar{Q}_{12} & \bar{Q}_{22} & \bar{Q}_{26} \\ \bar{Q}_{16} & \bar{Q}_{26} & \bar{Q}_{66} \end{bmatrix}_k \begin{bmatrix} \alpha_x \\ \alpha_y \\ \alpha_{xy} \end{bmatrix} \quad (4)$$

where ΔT is temperature change and $[\alpha]_k$ is the coefficient matrix of thermal expansion. The coefficients of thermal expansion (CTEs) of a composite lamina can be calculated by the following expression.

$$\begin{bmatrix} \alpha_x \\ \alpha_y \\ \alpha_{xy} \end{bmatrix}_{\Delta T=1} = \begin{bmatrix} \alpha_x \\ \alpha_y \\ \alpha_{xy} \end{bmatrix} \begin{bmatrix} A_{11}^* & A_{12}^* & A_{16}^* \\ A_{12}^* & A_{22}^* & A_{26}^* \\ A_{16}^* & A_{26}^* & A_{66}^* \end{bmatrix} \begin{bmatrix} N_x^T \\ N_y^T \\ N_{xy}^T \end{bmatrix} \quad (5)$$

in which $[A^*] = [A]^{-1}$.

It can be noted that the coefficient of thermal expansion must be 10^{-6} or less to achieve high dimensional stability in laminated composite structures.

3. Failure Criteria

In our study, several optimum laminate designs were selected at the end of the optimization to assess their dimensional stability considering the first ply failure under thermal loading conditions. For this purpose, Tsai-Wu and Hashin-Rotem failure criteria were used to analyze the strength of optimum stacking sequence designs subjected to thermal [17], [18].

3.1. Tsai-Wu Failure Criterion

The Tsai-Wu failure criterion based on total strain energy was derived from the von Mises yield criterion for laminated composite materials. According to the criterion, a lamina of a composite plate is considered to have failed if the following condition is satisfied:

$$F_1\sigma_1 + F_2\sigma_2 + F_6\tau_{12} + F_{11}\sigma_1^2 + F_{22}\sigma_2^2 + F_{66}\tau_{12}^2 + 2F_{12}\sigma_1\sigma_2 < 1 \quad (6)$$

where σ_1 and σ_2 are maximum normal stresses in fiber and transverse directions, respectively. τ_{12} is maximum shear stress.

Failure tensor expressions, F_{ij} ($i,j=1,2,6$) denoted in the equation are also given below.

$$\begin{aligned} F_1 &= \frac{1}{(\sigma_1^T)_{ult}} - \frac{1}{(\sigma_1^C)_{ult}}, F_2 = \frac{1}{(\sigma_2^T)_{ult}} - \frac{1}{(\sigma_2^C)_{ult}}, \\ F_{11} &= \frac{1}{(\sigma_1^T)_{ult}} - \frac{1}{(\sigma_1^C)_{ult}}, \\ F_{12} &= -\frac{1}{2} \sqrt{\frac{1}{(\sigma_1^T)_{ult} \cdot (\sigma_1^C)_{ult}} \cdot \frac{1}{(\sigma_2^T)_{ult} \cdot (\sigma_2^C)_{ult}}}, \\ F_{22} &= \frac{1}{(\sigma_2^T)_{ult} (\sigma_2^C)_{ult}}, \\ F_{66} &= \frac{1}{(\tau_{12})_{ult}^2} \end{aligned} \quad (7)$$

where $(\sigma_1^T)_{ult}$ is ultimate tensile strength in longitudinal direction, $(\sigma_1^C)_{ult}$ is compressive strength in longitudinal direction, $(\sigma_2^T)_{ult}$ is tensile strength in transverse direction, $(\sigma_2^C)_{ult}$ is compressive strength in transverse direction, and $(\tau_{12})_{ult}^2$ is ultimate shear strength.

3.2. Hashin-Rotem Failure Criterion

Fiber failure of tensile stress in unidirectional lamina ($\sigma_1 > 0$)

$$\sigma_1 = (\sigma_1^T)_{ult} \quad (8)$$

Fiber failure of compressive stress in unidirectional lamina ($\sigma_1 < 0$)

$$-\sigma_1 = (\sigma_1^C)_{ult} \quad (9)$$

Matrix failure of tensile stress in unidirectional lamina ($\sigma_2 > 0$)

$$\left(\frac{\sigma_2}{(\sigma_2^T)_{ult}}\right)^2 + \left(\frac{\tau_{12}}{(\tau_{12})_{ult}}\right)^2 = 1 \quad (10)$$

Matrix failure of compressive stress in unidirectional lamina ($\sigma_2 < 0$)

$$\left(\frac{\sigma_2}{(\sigma_2^C)_{ult}}\right)^2 + \left(\frac{\tau_{12}}{(\tau_{12})_{ult}}\right)^2 = 1 \quad (11)$$

4. Optimization

Stochastic optimization algorithms are generally preferred to solve the optimization problems of composite laminates since they are very capable of finding global optima in the problems, despite the more complex mathematical nature of composite materials than conventional materials. In this study, a hybrid algorithm consisting of a genetic algorithm (GA) and a generalized pattern search algorithm (GPSA) was used. The GA/GPSA hybrid algorithm was created using the MATLAB Optimization Toolbox [19].

Hybrid algorithms generally aim to create a new powerful algorithm by combining the superior features of two different algorithms and, thus, achieving the most accurate result in the optimization. Hybrid algorithms are used in many fields, such as engineering, for the solution of complex problems in the literature.

Genetic algorithm (GA) was discovered in 1975 by John Holland et al. It is a stochastic search method that carries Charles Darwin's theory of natural selection to the computer environment by modeling Darwin's theory of biological evolution, which is based on the survival of the best and aims to constantly reach the best [20]. GA aims to reach the optimum solution by determining the global optimum solution among more than one possible solution to a problem by determining the appropriate algorithm parameters [21]. GA randomly selects a population of individuals to begin its research. Each member of the population has a chromosome that encodes certain traits and assigns a degree of fitness according to specifications. This fitness rating is used to find designs that outperform their competitors. In the preceding step, the desired genetic material is used to protect a new part. This part pays off by applying more operators like genetic processing called gene crossover, gene mutation, and substitution. This process is repeated over many generations until the optimum value is achieved [22].

The second algorithm, the generalized pattern search algorithm (GPSA), was defined by Torczon [23] for the undifferentiated, unconstrained optimization of functions and then expanded to consider nonlinearly constrained optimization problems. GPSA approaches the most suitable point or points that will lead the problem to a global solution. Direct search does not require any gradient knowledge of the objective function and can be used to solve problems where the objective function is not differentiable, stochastic, or continuous.

The optimization method, which states how the hybrid algorithm GA used in the design works and interacts with GPSA, is given in Figure 2 and explained step by step.

Step 1. Starting with GA, all possible solutions in the search space are encoded as sequences.

Step 2. Usually, a random solution set is chosen and considered as the initial population.

Step 3. A fitness value is calculated for each array; the found fitness values show the solution quality of the arrays.

Step 4. A group of sequences is randomly selected according to a certain probability value, multiplication is performed, and the fitness values of the new individuals are calculated.

Step 5. The crossover operator is used to create new chromosomes with better qualities than the previous generation.

Step 6. The mutation operation generates new chromosomes from existing chromosomes.

Step 7. At the end of the GA, the optimal solution obtained is used as a starting point for the GPSA.

Step 8. GPSA starts the search with the first solution x_0 and obtains the initial mesh size Δ_0^m .

Step 9. In the search phase, if it finds a solution with an objective function value lower than the best solution, the algorithm stops.

Step 10. If the termination criteria are not met, the algorithm goes into the polling phase and creates a series of neighboring network points x_i^m by multiplying the current mesh size by each pattern vector $\{d_i\}$.

Step 11. Fixed directional pattern vectors, points to look for at each iteration used to clarify and define arguments in the objective function; the highest base with $2N$ vectors and the lowest base with $N+1$ vectors, usually consisting of N positive and B negative vectors.

Step 12. In the k th iteration step, GPSA probes all network points by calculating objective function values to find a satisfying point.

Step 13. If the polling was successful, that is, an improved point is found, it is multiplied by the existing mesh size, and this point is updated with the new mesh size for the next iteration $k+1$. An optimized point, the mesh size is reduced, and this current point is reused for the next iteration.

Step 14. This process continues with many iterations until the global optimum is reached. It is previously reported that the GA/GPSA hybrid algorithm finds better results compared to the previous results in the literature in test problems and shows very good performance in terms of speed and capability in searching design space for laminated composite problems [24].

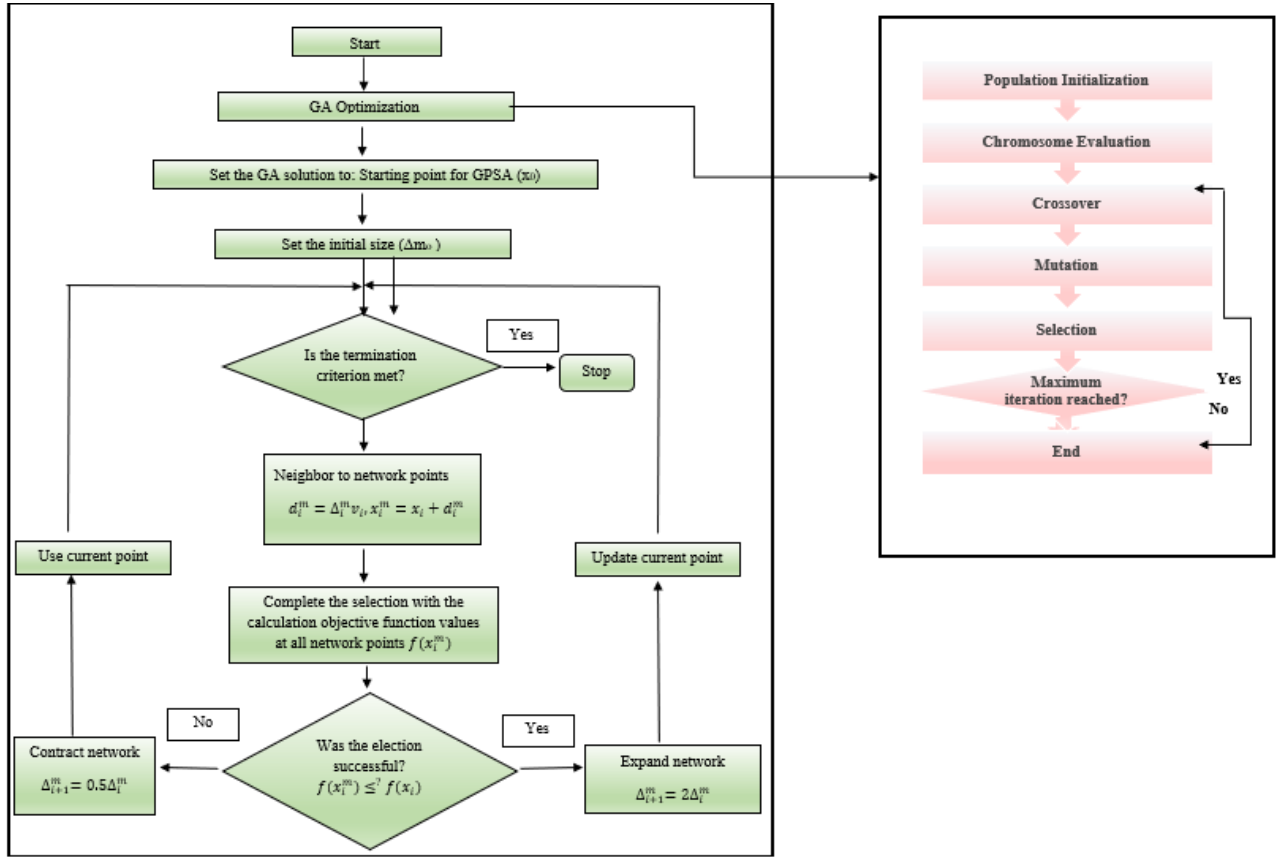


Figure 2. Flowchart of GA/GPSA hybrid algorithm

5. Problem Definition

The highest dimensional stability was investigated in hybrid composite laminates by minimizing the thermal expansion coefficients with the optimum stacking sequences. For this purpose, eight different

composite materials, Aramid/Epoxy, AS4/Epoxy, Boron/Epoxy, E-glass/Epoxy, IM6/Epoxy, GY70/Epoxy, Kevlar49/Epoxy, and Spectra/Epoxy were selected to hybridize the laminates [25], [26]. The mechanical properties of these materials are presented in Table 1.

Table 1. Material properties used in layered composite design

Material property	Spectra/Epoxy	E-Glass/Epoxy	Kevlar 49/Epoxy	AS4/Epoxy	IM6/Epoxy	Boron/Epoxy	GY70/Epoxy	Aramid/Epoxy
E_1 (GPa)	31	43	76	138	172	240	325	95
E_2 (GPa)	3.4	9.7	5.5	10.3	10.0	18.6	6.2	5.1
G_{12} (GPa)	1.4	6.2	2.1	6.9	6.2	6.6	5.2	1.8
ν_{12}	0.32	0.26	0.34	0.30	0.29	0.23	0.26	0.34
X_1^T (MPa)	1100	1070	1380	2275	2760	1590	760	2100
X_2^T (MPa)	8	38	30	52	50	60	26	1200
X_1^C (MPa)	83	870	275	1590	1540	2930	705	30
X_2^C (MPa)	48	185	138	207	152	200	70	130
S_6 (MPa)	24	72	43	131	124	108	27	30
$\alpha_1(10^{-6})/^\circ\text{C}$	-11	6.4	-2	-0.1	-0.4	4.5	-0.5	-3.6
$\alpha_2(10^{-6})/^\circ\text{C}$	120	16	57	18	18	20	1895	60

The optimization problems for this study can be stated in general as follows:

Find: $\{\theta_k, n\}, \{-90:90\} \wedge \{0,45,90\}, k = 1, \dots, n$

Minimize: α_x, α_y (single-objective functions)

Constraints: $[A/B]_{4S}, [A_4/B_4]_S$ material sequences

Algorithm: GA/GPSA hybrid algorithm (MATLAB Optimization Toolbox).

In the optimization problems, fiber angles as design variables in stacking sequences were considered as both continuous fiber angles ($-90^\circ:90^\circ$) and traditional fiber angles ($0^\circ, 45^\circ, 90^\circ$). Thus, the number of design variables, n becomes 8. A hybrid composite lay-up was applied as geometrical constraints in two different material sequences, with two selected materials represented as A and B. These material sequences are shown schematically in detail in Figures 3(a) and 3(b). The thickness of each layer was taken as 0.125 mm. For optimization problems, objective functions, which are coefficients of thermal expansion, are minimized, considering them as single-objective functions. As the problems are single objectives, when a minimum thermal expansion coefficient in one direction was found, the other thermal expansion coefficient in the other direction was calculated considering the optimum stacking sequence of the related laminate. Five different optimization scenarios for hybrid and non-hybrid composite designs were considered.

5.1. Non-hybrid Optimization

Before the hybrid composite material optimization, non-hybrid stacking sequence optimization of the composite materials was performed by using both the continuous fiber angles ($-90^\circ - 90^\circ$) and traditional fiber angles ($0^\circ, 45^\circ, 90^\circ$) to find the minimum thermal expansion coefficients (α_x and α_y) and compare them to the hybrid optimization results. The composite laminates were taken as 16-layer and symmetric in compliance with the hybrid problems.

5.2. Hybrid Optimization

In the optimization of hybrid composite plates, four optimization scenarios were considered, including both continuous and conventional fiber angles. These scenarios are briefly explained below:

Optimization scenario 1

In the first scenario, the $[A/B]_{4S}$ material sequence was considered for optimization, and the continuous

fiber angles ($-90^\circ - 90^\circ$) were used in the search for design variables of the problems. GY70/Epoxy and AS4/Epoxy composites were selected as the A materials in the sequence. The A materials were hybridized with the composite materials, the B materials, which are selected from Table 1.

Optimization scenario 2

In the second scenario, the $[A/B]_{4S}$ material sequence was taken into consideration with $0^\circ, 45^\circ, 90^\circ$ traditional fiber angles to investigate the minimums of thermal expansion coefficients of the hybrid composite laminates. GY70/Epoxy and AS4/Epoxy composites are the A materials in the sequence. These composite materials were hybridized with the B materials selected from Table 1.

Optimization scenario 3

In the third scenario, the $[A_4/B_4]_S$ material sequence was considered with the continuous fiber angles ($-90^\circ - 90^\circ$) to obtain the optimum stacking sequences of the dimensionally stable hybrid composite laminates. Similarly, GY70/Epoxy and AS4/Epoxy composites are specified as the A materials in the sequence, and these materials were hybridized with the other materials given in Table 1 as the B materials.

Optimization scenario 4

As a final optimization scenario, the $[A_4/B_4]_S$ material sequence was used by considering $0^\circ, 45^\circ, 90^\circ$ traditional fiber angles in the stacking sequence optimization to reach the dimensionally stable hybrid composite laminates. Similarly, GY70/Epoxy and AS4/Epoxy composites are the A materials in the sequence, and these composite materials were hybridized with the materials in Table 1 as the B materials.

Considering these optimization scenarios, 198 optimization problems, of which 16 were for non-hybrid laminated composites and 182 were for hybrid laminated composites, were solved in total.

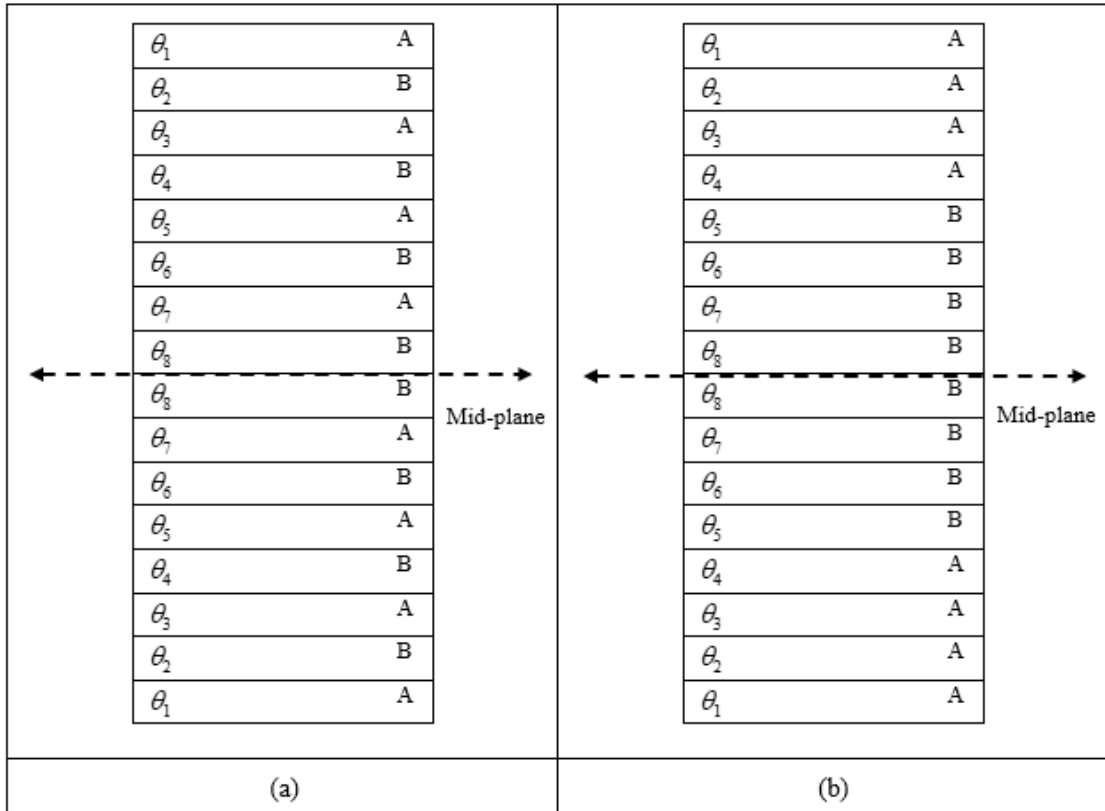


Figure 3. (a) Arrangement of 16-layered $[A/B]_{4S}$ hybrid composite plates (b) Arrangement of 16-layered $[A_4/B_4]_S$ hybrid composite plates

6. Results and Discussion

6.1. Optimization results

In the optimization, each problem was solved at least 100 times using the GA/GPSA hybrid algorithm created by the MATLAB program, and the results were presented in the tables. The result tables include material type, stacking sequence, minimized thermal expansion coefficients, and calculated thermal expansion coefficients. First, the non-hybrid composite laminate optimization results obtained using the continuous and traditional angles are given in Table 2 and Table 3, respectively. It should be noted that any result of a thermal expansion coefficient value below an order of 10^{-6} can be accepted as an optimum design in terms of dimensional stability [27].

It is seen in Table 2 that thermal expansion coefficients α_x and α_y were minimized to values in the order of $10^{-9} - 10^{-6}$ for AS4/Epoxy, IM6/Epoxy, Spectra/Epoxy, and Boron/Epoxy non-hybrid composites with the optimum continuous angled designs. In the other materials, the minimum values were mostly obtained in the order of 10^{-6} .

In Table 3, it can be noted that α_x and/or α_y could be minimized to the order of 10^{-8} at most for the model problems AS4/Epoxy, IM6/Epoxy, Gy70/Epoxy, and Boron/Epoxy with the optimum traditional angled designs. It can be said that these thermal expansion coefficient values are smaller as compared to those obtained by the continuous-angled designs. The results of optimization scenarios 1 – 4, including hybrid composite plates, are presented in Tables 4 – 11. The results of optimization scenario 1 are given in Tables 4 and 5.

Table 2. Optimization results of the continuous angled non-hybrid composite plates

Opt.	Composite	Stacking sequence	α_x (1/°C)	α_y (1/°C)
Min α_x	E-Glass/ Epoxy	[19 ₄ /86/16/1/75] _s	8.0417.10 ⁻⁶	1.0595.10 ⁻⁵
Min α_y		[73/90 ₇] _s	1.5816.10 ⁻⁵	6.3947.10 ⁻⁶
Min α_x	Kevlar49/Epoxy	[84/81/88/59/83/89/82/62] _s	4.1884.10 ⁻⁶	-7.5086.10 ⁻⁷
Min α_y		[89/70/67/75/86/67/71/82] _s	6.3444.10 ⁻⁶	-2.9069.10 ⁻⁶
Min α_x	AS4/ Epoxy	[10/14/0/30/0/2/82/84] _s	5.3587.10 ⁻⁶	1.1134.10 ⁻⁶
Min α_y		[58/44/28/90/34/90/21/26] _s	1.3947.10 ⁻⁶	-2.7594.10 ⁻⁷
Min α_x	IM6/ Epoxy	[79/61/8/88/79/75/88 ₂] _s	3.2160.10 ⁻⁸	3.2160.10 ⁻⁷
Min α_y		[63/89 ₂ /76/87/63/74/87] _s	1.2026.10 ⁻⁸	1.2026.10 ⁻⁸
Min α_x	GY70/Epoxy	[88/49/66/58/85/89/90 ₂] _s	1.4244.10 ⁻⁶	-3.2458.10 ⁻⁷
Min α_y		[88/49/66/59/85/90 ₃] _s	1.4183.10 ⁻⁶	-3.2458.10 ⁻⁷
Min α_x	Aramid/ Epoxy	[65/81/73/7/16/65/14/31] _s	3.5661.10 ⁻⁶	-4.1119.10 ⁻⁸
Min α_y		[41/9/73/50/59/42/81] _s	7.1708.10 ⁻⁸	3.4533.10 ⁻⁶
Min α_x	Spectra/ Epoxy	[21/82/5/60/19/12/42/11] _s	6.8621.10 ⁻⁶	-4.9593.10 ⁻⁸
Min α_y		[56/28/20/30/42/66/83/86] _s	6.8260.10 ⁻⁶	-1.3531.10 ⁻⁸
Min α_x	Boron/ Epoxy	[26/51/39/68/20/55/62] _s	1.4421.10 ⁻⁸	1.5168.10 ⁻⁶
Min α_y		[74/50/30/14/69/5/36/5] _s	1.5299.10 ⁻⁶	1.3757.10 ⁻⁹

Table 3. Optimization results of the traditional angled non-hybrid composite plates

Opt.	Composite	Stacking sequence	α_x (1/°C)	α_y (1/°C)
Min α_x	E-Glass/ Epoxy	[0 ₃ /45 ₅] _s	7.6030.10 ⁻⁶	1.2081.10 ⁻⁵
Min α_y		[90 ₄ /45/90 ₂] _s	1.4571.10 ⁻⁵	6.4999.10 ⁻⁶
Min α_x	Kevlar49 / Epoxy	[0/90 ₇] _s	-1.2500.10 ⁻⁷	3.5625.10 ⁻⁶
Min α_y		[90 ₆ /45/90] _s	3.5625.10 ⁻⁶	-2.500.10 ⁻⁷
Min α_x	AS4/ Epoxy	[45 ₈] _s	5.5937.10 ⁻⁷	5.5938.10 ⁻⁷
Min α_y		[90 ₅ /45/90/45] _s	1.1965.10 ⁻⁶	-7.7743.10 ⁻⁶
Min α_x	IM6/ Epoxy	[0/90 ₇] _s	-2.5000.10 ⁻⁶	1.1250.10 ⁻⁶
Min α_y		[90 ₈] _s	1.1250.10 ⁻⁶	-2.5000.10 ⁻⁶
Min α_x	GY70/ Epoxy	[45 ₈] _s	5.4687.10 ⁻⁷	5.4687.10 ⁻⁷
Min α_y		[90 ₈] _s	1.1250.10 ⁻⁶	-3.1250.10 ⁻⁸
Min α_x	Aramid/ Epoxy	[45 ₈] _s	1.7625.10 ⁻⁶	1.7625.10 ⁻⁶
Min α_y		[90 ₈] _s	3.7500.10 ⁻⁶	-2.2500.10 ⁻⁷
Min α_x	Spectra/ Epoxy	[0/90 ₇] _s	-6.8750.10 ⁻⁷	7.5000.10 ⁻⁶
Min α_y		[90 ₈] _s	7.5000.10 ⁻⁶	-6.8750.10 ⁻⁶
Min α_x	Boron/ Epoxy	[0/45 ₂ /90 ₃ /90/45/90] _s	1.5818.10 ⁻⁸	1.5154.10 ⁻⁶
Min α_y		[90/45 ₂ /90/45/90 ₃] _s	1.5154.10 ⁻⁶	1.5818.10 ⁻⁸

Table 4 shows the results of the stacking sequence with continuous fiber angles for the [A/B]_{4s} hybrid laminates of GY70/Epoxy material. Most of the designs with thermal expansion coefficients in the order of 10⁻⁷ – 10⁻⁹ were achieved. The lowest α_x value giving minimum dimensional change is

obtained as 1.1924·10⁻⁸ 1/°C for the GY70-IM6/Epoxy hybrid composite, and the lowest α_x value giving minimum dimensional change is obtained as 1.1932·10⁻⁹ 1/°C for the GY70-Spectra/Epoxy hybrid composite.

Table 5 presents the results of the stacking sequence with continuous fiber angles for the $[A/B]_{4s}$ hybrid laminates of AS4/Epoxy material. As seen in Table 5, it is observed that the α_x value was minimized to the order of 10^{-10} , and the α_y value is minimized to the order of 10^{-8} at most. Hence, more

dimensionally stable hybrid laminates were obtained when the x direction value was minimized to the order of 10^{-10} , and the α_y value was minimized to the order of 10^{-8} at most. Hence, more dimensionally stable hybrid laminates were obtained in the x direction compared to the y direction.

Table 4. $[A/B]_{4s}$ optimization results of hybrid composite plates with the continuous angles (A - GY70/Epoxy)

Opt.	Hybrid Composite	Stacking Sequence	α_x (1/°C)	α_y (1/°C)
Min α_x	GY70-Spectra/Epoxy	[5/75/69 ₂ /0 ₂ /1/72] _s	2.6534.10 ⁻⁸	3.8923.10 ⁻⁵
Min α_y		[67/41/37/78/89/46/76/40] _s	3.8949.10 ⁻⁵	1.1932.10 ⁻⁹
Min α_x	GY70-Kevlar 49/Epoxy	[25/65/90/68/33/63/12/5] _s	-2.2366.10 ⁻⁸	1.4153.10 ⁻⁵
Min α_y		[3/25/54/76/16/43/29/84] _s	1.4104.10 ⁻⁵	2.7420.10 ⁻⁸
Min α_x	GY70-IM6/Epoxy	[41/8/52/23/51/8/27/26] _s	1.1924.10 ⁻⁶	1.1385.10 ⁻⁶
Min α_y		[90/35 ₂ /7/64/39/42/44] _s	1.1401.10 ⁻⁵	3.8628.10 ⁻⁹
Min α_x	GY70- E-Glass/Epoxy	[3/43/18/74/22/64/23/38] _s	-1.8190.10 ⁻⁸	1.3181.10 ⁻⁶
Min α_y		[28/5/20/7/29/14/20/22] _s	1.3108.10 ⁻⁶	1.8696.10 ⁻⁸
Min α_x	GY70-AS4/Epoxy	[82/10/37/9/84/54/83/48] _s	8.0163.10 ⁻⁷	-1.2367.10 ⁻⁸
Min α_y		[1/0/1/2/0 ₃ /-1] _s	3.1808.10 ⁻⁸	5.3994.10 ⁻⁶
Min α_x	GY70-Aramid/Epoxy	[49/36/49/67/73/35/46/31] _s	-2.5290.10 ⁻⁷	1.4687.10 ⁻⁵
Min α_y		[89/80/22/80/0/88/60/67] _s	1.4385.10 ⁻⁵	4.9351.10 ⁻⁸
Min α_x	GY70- Boron/Epoxy	[41/80/46/79/49/64/4/85] _s	4.6718.10 ⁻⁷	2.4544.10 ⁻⁶
Min α_y		[72/14/63/33/72/6/65/2] _s	2.6204.10 ⁻⁶	-4.2191.10 ⁻⁹

Table 5. $[A/B]_{4s}$ optimization results of hybrid composite plates with the continuous angles (A - AS4/Epoxy)

Opt.	Hybrid Composite	Stacking Sequence	α_x (1/°C)	α_y (1/°C)
Min α_x	AS4-Spectra/Epoxy	[19/1/0/1/0/1/-1/1] _s	-1.1329.10 ⁻⁸	1.4595.10 ⁻⁵
Min α_y		[49/10/85/31/71/28/87/54] _s	1.4540.10 ⁻⁵	4.3517.10 ⁻⁸
Min α_x	AS4-E-Glass/Epoxy	[39/89/42/3/42/84/39/83] _s	-5.4662.10 ⁻⁹	2.6115.10 ⁻⁶
Min α_y		[50/4/53/4/50/4/50/4] _s	1.2729.10 ⁻⁶	1.4327.10 ⁻⁶
Min α_x	AS4-IM6/Epoxy	[1/2/1/-1/2/0/2/1] _s	8.4299.10 ⁻⁹	7.9839.10 ⁻⁶
Min α_y		[77/38/80/70/54/18/67/5] _s	8.0075.10 ⁻⁶	-1.5086.10 ⁻⁸
Min α_x	AS4-GY70/Epoxy	[1/86/1/2/1/-1 ₂ /0] _s	6.4736.10 ⁻⁹	5.3934.10 ⁻⁶
Min α_y		[74/50/73/77/69/1438/34] _s	5.4123.10 ⁻⁶	-1.2453.10 ⁻⁸
Min α_x	As4-Kevlar49/Epoxy	[89/-1/1/0 ₃ /7/2] _s	-3.4388.10 ⁻¹⁰	1.1534.10 ⁻⁵
Min α_y		[55/30/62/50/80/51/64/90] _s	1.1512.10 ⁻⁵	2.1798.10 ⁻⁸
Min α_x	AS4-Aramid/Epoxy	[47/54/19/0/66/3/20/10] _s	4.7703.10 ⁻⁸	2.4953.10 ⁻⁵
Min α_y		[90/77/53/69/51/77/43/38] _s	2.4941.10 ⁻⁵	6.0218.10 ⁻⁸
Min α_x	AS4-Boron/Epoxy	[45/90/45/82/45/90/45/82] _s	1.7397.10 ⁻⁶	3.3066.10 ⁻⁶
Min α_y		[45/-17/45/-17/45/17/45/17] _s	3.3878.10 ⁻⁶	1.7243.10 ⁻⁶

The results of optimization scenario 2 were given in Tables 6 and 7. Table 6 shows the results of the optimum stacking sequences with traditional 0°, 45°, and 90° fiber angles for the [A/B]_{4S} hybrid laminates of GY70/Epoxy. As seen in Table 6, most of the designs with thermal expansion coefficients in the order of 10⁻⁷ – 10⁻⁸ were obtained. The best thermal expansion coefficient value of α_x for dimensional stability was achieved in GY70-E-Glass/ Epoxy hybrid composite with 7.9853·10⁻⁸ 1/°C. For the thermal expansion coefficient of (α_y), the best dimensional stability was reached in GY70-AS4/Epoxy with a value of 3.5850·10⁻⁸ 1/°C. Furthermore, it is seen that more optimum stacking sequences with lower thermal expansion coefficients were obtained in the y direction of the laminates than in the x direction in terms of dimensional stability. Table 7 indicates the results of the stacking sequences with the traditional fiber angles for the [A/B]_{4S} hybrid laminates of AS4/Epoxy.

It is noticed that the coefficients of thermal expansion (CTEs) were mainly obtained in the order of 10⁻⁸ in the optimization problems. Moreover, lower CTE values were found for the α_y compared to the α_x . However, it is seen that the desired

dimensional stability could not be reached for the AS4-Boron/Epoxy hybrid laminate design cases.

Considering the dimensionally stable hybrid designs of the traditional fiber and continuous fiber angles (optimization scenario 1 and 2) comparatively, it can be said that the trend of finding lower CTE is higher in the hybrid designs with the continuous fiber angles, as can be expected. However, it is seen that the hybrid laminate optimization with the traditional angles yielded competitive results in several cases as well.

On the other hand, when all continuous angled-hybrid designs are compared with continuous-angled non-hybrid designs, it can be interpreted that the dimensional stability performances of the hybrid designs are mainly at a better level than the non-hybrid designs. However, considering the comparison of the traditional angled hybrid and non-hybrid designs, it is seen that IM6/Epoxy and Boron/Epoxy non-hybrid composites provided better results alone than most of the hybrid designs. Furthermore, unexpectedly, the α_x values were obtained lower in the non- hybrid designs of GY70/Epoxy compared to its hybrid designs, and the α_y values were obtained lower in the non-hybrid designs of AS4/Epoxy compared to its hybrid designs.

Table 6. [A/B]_{4S} optimization results of hybrid composite plates with the traditional angles (A - GY70/Epoxy)

Opt.	Hybrid Composite	Stacking Sequence	α_x (1/°C)	α_y (1/°C)
Min α_x	Gy70-Spectra/Epoxy	[0/45 ₇] _S	-2.1054.10 ⁻⁷	1.6145.10 ⁻⁵
Min α_y		[90/45/90/0/45/0/45/0] _S	1.5838.10 ⁻⁵	9.6472.10 ⁻⁸
Min α_x	GY70-Kevlar 49/Epoxy	[45 ₄ /90/45 ₂ /0] _S	-3.6668.10 ⁻⁷	1.4168.10 ⁻⁵
Min α_y		[90 ₄ /45/90 ₃] _S	1.4168.10 ⁻⁵	-3.6818.10 ⁻⁸
Min α_x	Gy70-E-Glass/Epoxy	[45 ₃ /90/45 ₃ /90] _S	7.9853.10 ⁻⁸	1.2666.10 ⁻⁶
Min α_y		[45/0/45/0/45/0/90/0] _S	1.2028.10 ⁻⁶	1.1590.10 ⁻⁷
Min α_x	Gy70-IM6/Epoxy	[0/90/0/90/0/90/45/90] _S	2.8254.10 ⁻⁷	1.1114.10 ⁻⁵
Min α_y		[45 ₄ /90 ₄] _S	1.1504.10 ⁻⁵	-1.0670.10 ⁻⁷
Min α_x	Gy70-AS4/Epoxy	[45 ₈] _S	2.6999.10 ⁻⁶	2.6999.10 ⁻⁶
Min α_y		[90 ₈] _S	5.3640.10 ⁻⁶	3.5850.10 ⁻⁸
Min α_x	Gy70-Aramid/Epoxy	[0/45 ₂ /0/45 ₃ /0] _S	-4.0097.10 ⁻⁷	2.8601.10 ⁻⁵
Min α_y		[45/90/45 ₂ /90/45 ₃] _S	2.8601.10 ⁻⁵	-4.0097.10 ⁻⁷
Min α_x	Gy70-Boron/Epoxy	[45/90/45 ₃ /90] _S	2.8872.10 ⁻⁶	2.5032.10 ⁻⁶
Min α_y		[45/0/45/0/45/0/90/0] _S	9.1449.10 ⁻⁸	3.6559.10 ⁻⁷

Table 7. [A/B]_{4S} optimization results of hybrid composite plates with the traditional angles (A - AS4/Epoxy)

Opt.	Hybrid Composite	Stacking Sequence	α_x (1/°C)	α_y (1/°C)
Min α_x	AS4- Spectra/Epoxy	[0/90/0/45 ₅] _S	1.8388.10 ⁻⁸	1.4565.10 ⁻⁵
Min α_y		[45/0/90/45/90/45 ₃] _S	14565.10 ⁻⁵	1.8388.10 ⁻⁸
Min α_x	AS4-E-Glass/Epoxy	[45/90] _{4S}	-3.9553.10 ⁻⁸	2.6416.10 ⁻⁶
Min α_y		[45/0] _{4S}	2.6416.10 ⁻⁶	-3.9553.10 ⁻⁸
Min α_x	AS4-Kevlar 49/Epoxy	[90/45 ₃ /90/45 ₂ /0] _S	-2.9896.10 ⁻⁷	1.1833.10 ⁻⁵
Min α_y		[90 ₈] _S	-7.3619.10 ⁻⁵	1.1608.10 ⁻⁸
Min α_x	AS4- IM6/Epoxy	[45/90/45 ₆] _S	8.0512.10 ⁻⁷	7.1873.10 ⁻⁶
Min α_y		[90 ₈] _S	8.0123.10 ⁻⁶	-1.9915.10 ⁻⁸
Min α_x	AS4- GY70/Epoxy	[45 ₈] _S	2.6999.10 ⁻⁶	2.6999.10 ⁻⁶
Min α_y		[90 ₈] _S	5.3640.10 ⁻⁶	3.5850.10 ⁻⁸
Min α_x	AS4-Aramid/Epoxy	[90/45 ₆ /0] _S	3.2255.10 ⁻⁷	3.9063.10 ⁻⁵
Min α_y		[0/45 ₂ /90 ₄] _S	3.9063.10 ⁻⁵	3.2255.10 ⁻⁷
Min α_x	AS4-Boron/Epoxy	[45/90] _{4S}	1.7403.10 ⁻⁶	3.2993.10 ⁻⁶
Min α_y		[45/0] _{4S}	3.2993.10 ⁻⁶	1.7403.10 ⁻⁶

The results of optimization scenario 3 are given in Tables 8 and 9. Table 8 shows the results of the optimum stacking sequences with the continuous fiber angles for the [A/B]_{4S} hybrid laminates of GY70/Epoxy, and Table 9 presents the results of the continuous fiber-angled hybrid designs for the [A/B]_{4S} hybrid laminates of AS4/Epoxy. As seen in Table 8, in most of the designs, thermal expansion coefficients have been obtained in the order of 10⁻⁷ –

10⁻⁹. The lowest α_x value was obtained with GY70-Kevlar49/Epoxy hybrid design as 4.3532·10⁻⁹ 1/°C, and the lowest α_y value was obtained as 3.3355·10⁻⁹ 1/°C in the GY70-E-Glass/Epoxy hybrid design. However, any optimum design that provides better dimensional stability in both directions could not be reached with the GY70-Boron/Epoxy design.

Table 8. [A/B]_{4S} optimization results of hybrid composite plates with the continuous angles (A - GY70/Epoxy)

Opt.	Hybrid Composite	Stacking Sequence	α_x (1/°C)	α_y (1/°C)
Min α_x	GY70-Spektra /Epoxy	[4/23/11/36/38/32/43/67] _S	-3.9410.10 ⁻⁸	-1.5974.10 ⁻⁵
Min α_y		[55/72/83/88/19/45/70/62] _S	1.5961.10 ⁻⁵	-2.6662.10 ⁻⁸
Min α_x	GY70-Kevlar49/Epoxy	[1 ₂ /0/29/1/2 ₂ /1] _S	4.3532.10 ⁻⁹	1.4127.10 ⁻⁶
Min α_y		[84 ₂ /56/52/42/63/5/57] _S	1.4114.10 ⁻⁵	1.6471.10 ⁻⁸
Min α_x	GY70-E-Glass/Epoxy	[25/80/57/45/36/16/57/71] _S	-7.4635.10 ⁻⁸	1.6722.10 ⁻⁶
Min α_y		[0/84/89/36/49/46/48/5] _S	1.6799.10 ⁻⁶	3.3555.10 ⁻⁹
Min α_x	GY70- IM6/Epoxy	[5/58/6/0 ₂ /83/56/38] _S	4.1138.10 ⁻⁸	1.1356.10 ⁻⁵
Min α_y		[73/80/77/53/36/72/89/28] _S	1.1334.10 ⁻⁵	6.3394.10 ⁻⁸
Min α_x	GY70- AS4/Epoxy	[82/10/37/9/84/54/83/48] _S	8.0163.10 ⁻⁷	-1.2367.10 ⁻⁸
Min α_y		[1/0/1/2/0 ₃ /-1] _S	3.1808.10 ⁻⁸	5.3994.10 ⁻⁶
Min α_x	GY70-Aramid/Epoxy	[37/21/48/61/82/6/50/37] _S	1.1212.10 ⁻⁷	2.8088.10 ⁻⁵
Min α_y		[56/65/15/78/35/85/75/36] _S	2.8290.10 ⁻⁵	-8.9561.10 ⁻⁸
Min α_x	GY70- Boron/Epoxy	[45/32/60/48/0/21/16/12] _S	1.9348.10 ⁻⁶	1.1787.10 ⁻⁸
Min α_y		[20/25/19/22/48/78/76/63] _S	1.4528.10 ⁻⁶	25505.10 ⁻⁶

In Table 9, it can be noted that high dimensional stability at adequate levels was met in almost all design cases, and the CTE values were obtained generally in the order of $10^{-8} - 10^{-10}$. The hybrid designs of Spectra/Epoxy, Kevlar 49/Epoxy, and E-Glass/Epoxy composites are better in terms of

dimensional stability than the other designs. However, similarly as in the hybrid of GY70/Epoxy, an optimum design solution for high dimensional stability also could not be found in the AS4-Boron/Epoxy hybrid composite.

Table 9. $[A_4/B_4]_s$ optimization results of hybrid composite plates with the continuous angles (A - AS4/Epoxy)

Opt.	Hybrid Composite	Stacking Sequence	α_x (1/ °C)	α_y (1/ °C)
Min α_x	AS4-Spectra/Epoxy	[61/56/88 ₂ /7/36/88/34] _s	8.4239.10 ⁻¹⁰	1.4587.10 ⁻⁵
Min α_y		[1/28/0 ₂ /1/21/1/0] _s	1.4582.10 ⁻⁵	-3.7348.10 ⁻⁹
Min α_x	AS4-Kevlar 49/Epoxy	[7/0/1 ₂ /0/-1/0 ₂] _s	1.4736.10 ⁻⁸	1.1519.10 ⁻⁵
Min α_y		[66/88/48/68/41/1/22/19] _s	1.1558.10 ⁻⁵	-2.3927.10 ⁻⁸
Min α_x	As4-IM6/Epoxy	[2/0/2 ₂ /1/0/2/-1] _s	8.5961.10 ⁻⁹	7.9838.10 ⁻⁶
Min α_y		[42/78/90/87/70/31/37] _s	8.2459.10 ⁻⁶	-2.5348.10 ⁻⁷
Min α_x	AS4-GY70/Epoxy	[31/22/14/6/39/72/1/18] _s	2.0431.10 ⁻⁹	5.3978.10 ⁻⁶
Min α_y		[1/0 ₃ /84/3/0 ₂] _s	-3.8115.10 ⁻⁹	5.4036.10 ⁻⁶
Min α_x	AS4-E-Glass/Epoxy	[40/43/40 ₂ /88/83/76/87] _s	1.7913.10 ⁻⁹	2.6082.10 ⁻⁶
Min α_y		[51/50/52 ₂ /4 ₃ /8] _s	2.6075.10 ⁻⁶	-3.7028.10 ⁻⁹
Min α_x	AS4-Aramid/Epoxy	[51/32/86/46/65/4/44/48] _s	1.1744.10 ⁻⁸	3.9374.10 ⁻⁷
Min α_y		[36/57/43/77/69/52/90/80] _s	3.9461.10 ⁻⁵	-7.5021.10 ⁻⁸
Min α_x	AS4- Boron/Epoxy	[45 ₄ /90/82 ₂ /90] _s	1.7397.10 ⁻⁶	3.3066.10 ⁻⁶
Min α_y		[45 ₄ /-18 ₄] _s	1.7619.10 ⁻⁶	3.3415.10 ⁻⁶

The results of optimization scenario 4 were presented in Tables 10 and 11. Tables 10 and 11 show the results of the optimum stacking sequence

designs with the traditional fiber angles for the $[A/B]_{4s}$ hybrid laminates of GY70/Epoxy and AS4/Epoxy, respectively.

Table 10. $[A_4/B_4]_s$ optimization results of hybrid composite plates with the traditional angles (A -GY70/Epoxy)

Opt.	Hybrid Composite	Stacking Sequence	α_x (1/ °C)	α_y (1/ °C)
Min α_x	Gy70-Spectra/Epoxy	[0/45 ₇] _s	-2.1054.10 ⁻⁷	1.6145.10 ⁻⁵
Min α_y		[45/90 ₂ /45/9045/90 ₂] _s	1.5838.10 ⁻⁵	9.6472.10 ⁻⁸
Min α_x	GY70-Kevlar 49/Epoxy	[0/45 ₃ /90/45 ₃] _s	2.8727.10 ⁻⁷	1.3844.10 ⁻⁵
Min α_y		[45/90 ₃ /0 ₄] _s	1.4092.10 ⁻⁷	3.8510.10 ⁻⁸
Min α_x	GY70-E-Glass/Epoxy	[90 ₂ /45 ₃ /90] _s	6.5897.10 ⁻⁹	1.7011.10 ⁻⁶
Min α_y		[45 ₆ /90/45] _s	1.4399.10 ⁻⁶	3.9905.10 ⁻⁸
Min α_x	GY70- IM6/Epoxy	[0 ₃ /45/90 ₄] _s	2.8254.10 ⁻⁷	1.1114.10 ⁻⁵
Min α_y		[45 ₂ /90 ₃ /45 ₂ /90] _s	1.1504.10 ⁻⁵	-1.0670.10 ⁻⁷
Min α_x	GY70-AS4/Epoxy	[45 ₈] _s	2.6999.10 ⁻⁶	2.6999.10 ⁻⁶
Min α_y		[90 ₈] _s	53640.10 ⁻⁶	3.5850.10 ⁻⁸
Min α_x	GY70-Aramid/Epoxy	[90 ₂ /45/90/0 ₄] _s	-4.3333.10 ⁻⁷	1.4868.10 ⁻⁵
Min α_y		[90 ₂ /45/90 ₅] _s	1.4868.10 ⁻⁵	-4.3333.10 ⁻⁷
Min α_x	GY70- Boron/Epoxy	[45 ₄ /90/45/90/45] _s	1.5102.10 ⁻⁶	2.8872.10 ⁻⁶
Min α_y		[45 ₃ /90/0 ₄] _s	1.8574.10 ⁻⁶	3.6559.10 ⁻⁷

Table 11. $[A_4/B_4]_s$ optimization results of hybrid composite plates with the traditional angles (A - AS4/Epoxy)

Opt.	Hybrid Composite	Stacking Sequence	α_x	α_y
			($1/^\circ\text{C}$)	($1/^\circ\text{C}$)
Min α_x	AS4-Spektra/Epoxy	$[0_245_2/90/45_3]_s$	$1.4565 \cdot 10^{-8}$	$1.8388 \cdot 10^{-5}$
Min α_y		$[45/90_2/45/90/45_3]_s$	$1.8388 \cdot 10^{-5}$	$1.4565 \cdot 10^{-8}$
Min α_x	AS4Kevlar 49/Epoxy	$[0/45_7]_s$	$-5.5543 \cdot 10^{-7}$	$-1.2090 \cdot 10^{-5}$
Min α_y		$[90_8]_s$	$1.1608 \cdot 10^{-5}$	$-7.3619 \cdot 10^{-8}$
Min α_x	AS4- E-Glass/Epoxy	$[45/90]_{4s}$	$-3.9553 \cdot 10^{-8}$	$2.6416 \cdot 10^{-6}$
Min α_y		$[45/0]_{4s}$	$2.6416 \cdot 10^{-6}$	$-3.9553 \cdot 10^{-8}$
Min α_x	AS4-IM6/Epoxy	$[0/45_3/90/45_3]_s$	$8.0512 \cdot 10^{-7}$	$7.1873 \cdot 10^{-6}$
Min α_y		$[90_8]_s$	$8.0123 \cdot 10^{-6}$	$-1.9915 \cdot 10^{-8}$
Min α_x	AS4-GY70/Epoxy	$[45_8]_s$	$2.6999 \cdot 10^{-6}$	$2.6999 \cdot 10^{-6}$
Min α_y		$[90_8]_s$	$5.3640 \cdot 10^{-6}$	$3.5850 \cdot 10^{-8}$
Min α_x	AS4-Aramid/Epoxy	$[90_4/0_4]_s$	$8.8268 \cdot 10^{-7}$	$2.4118 \cdot 10^{-5}$
Min α_y		$[90_8]_s$	$2.4118 \cdot 10^{-5}$	$8.8268 \cdot 10^{-7}$
Min α_x	AS4-Boron/Epoxy	$[45_4/90_4]_s$	$1.7403 \cdot 10^{-6}$	$3.2993 \cdot 10^{-6}$
Min α_y		$[45_4/0_4]_s$	$3.2993 \cdot 10^{-6}$	$1.7403 \cdot 10^{-6}$

It is seen from Table 10 that the dimensional stability performance of the GY70/Epoxy hybrid composites has been improved in the order of $10^{-7} - 10^{-9}$ in most of the design problems except for the GY70-Boron/Epoxy hybrid design. Besides, the performance of the dimensional stability of the AS4/Epoxy hybrids (Table 11) has also been improved to the order of 10^{-8} in many problems except for the AS4-Boron/Epoxy hybrid composite.

If the hybrid designs of the continuous fiber angles are compared to the designs of the traditional fiber angles (optimization scenarios 3 and 4), it is seen that the trend of finding lower CTE is higher in the hybrid designs with the continuous fiber angles, which is similar to the design cases in the optimization scenarios 1 and 2. In particular, the CTE values of the hybrid designs of AS4/Epoxy with the continuous angles were obtained lower (in the order of 10^{-9} and 10^{-10}) than the hybrid designs of GY70/Epoxy (in the order of 10^{-8} and 10^{-9}).

On the other hand, considering hybrid and non-hybrid designs of the continuous angled laminates, all the optimum designs of the GY70/Epoxy hybrids provide lower CTE values compared to the non-hybrid GY70/Epoxy design. However, the hybrid designs of GY70/Epoxy could not reach the minimum CTE values, in which min α_x was obtained by the non-hybrid AS4/Epoxy design and min α_y was obtained by the non-hybrid Boron/Epoxy design. When the hybrid designs of AS4/Epoxy are compared with the non-hybrid

designs of AS4/Epoxy, it is seen that α_y values are lower in all the hybrid designs; however, α_x values are lower in hybrid designs of AS4-Spektra/Epoxy, AS4-GY70/Epoxy, and AS4-E-Glass/Epoxy. Regarding the comparison of the AS4/Epoxy hybrid designs and the other non-hybrid designs, α_x values were obtained lower in of AS4-Spektra/Epoxy, AS4-GY70/Epoxy, and AS4-E-Glass/Epoxy composites as compared to the best min α_x value of the non-hybrid designs other than AS4/Epoxy. However, any optimum designs of min α_y were not found by any of the hybrids of AS4/Epoxy, considering the min α_y non-hybrid designs of materials other than AS4/Epoxy.

Considering the comparison of hybrid and non-hybrid designs of the traditional angled laminates, it can be said that all the designs of the GY70/Epoxy hybrids provided higher dimensional stability compared to the non-hybrid GY70/Epoxy design, which is similar to the continuous case. If the AS4/Epoxy hybrid designs are compared to the AS4/Epoxy non-hybrid designs, it can be noted that AS4-Spektra/Epoxy, AS4-Kevlar 49/Epoxy, and AS4-E-Glass/Epoxy hybrid designs ensured lower CTE values than the non-hybrid design for min α_x optimization. However, only AS4-Kevlar 49/Epoxy yielded a lower CTE value in min α_y optimization. Considering the comparison of AS4/Epoxy hybrids and the non-hybrid designs other than AS4/Epoxy, better CTE values were obtained for only the AS4-Spektra/Epoxy hybrid design for both minimum α_x

and α_y .

It is also important to compare the results of optimum continuous and traditional angled hybrid laminate designs of the $[A/B]_{4S}$ sequence with the results of the $[A_4/B_4]_S$ sequence. In continuous angled designs, for the min α_x optimization of GY70/Epoxy hybrids, all the designs of $[A/B]_{4S}$ sequence provide better dimensional stability than the designs of $[A_4/B_4]_S$ sequence, except GY70-Kevlar 49/Epoxy laminate. For the min α_y optimization of GY70/Epoxy, all the hybrid designs of the $[A/B]_{4S}$ sequence yield higher dimensional stability than the designs of the $[A_4/B_4]_S$ sequence, apart from the GY70-Kevlar 49/Epoxy and GY70-E-Glass/Epoxy designs.

In the AS4/Epoxy hybrid designs, AS4-Spectra/Epoxy, AS4-E-Glass/Epoxy, AS4-GY70/Epoxy, and AS4-Aramid/Epoxy laminates give lower CTE values of α_x in the $[A_4/B_4]_S$ sequence than the $[A/B]_{4S}$ sequence. Besides, AS4-Kevlar 49/Epoxy, AS4-IM6/Epoxy, and AS4-Boron/Epoxy laminate designs of the $[A_4/B_4]_S$ sequence yield smaller CTE values of α_x compared to the $[A_4/B_4]_S$ sequence. On the other hand, it is seen for the min α_y optimization that the hybrid designs of the $[A/B]_{4S}$ sequence provide better dimensional stability except for AS4-Spectra/Epoxy and AS4-E-Glass/Epoxy laminates than the designs of the $[A_4/B_4]_S$ sequence.

Considering the traditional angled case, for the min α_x optimization cases, the GY70/Epoxy hybrid laminate designs of Spectra/Epoxy and IM6/Epoxy give the same results for both $[A/B]_{4S}$ and $[A_4/B_4]_S$ sequences. The hybrid designs of GY70-Kevlar 49/Epoxy and GY70-E-Glass/Epoxy show higher dimensional stability in the $[A_4/B_4]_S$ sequence than the $[A/B]_{4S}$ sequence. However, the optimum GY70-Aramid/Epoxy design has lower CTE and thus higher dimensional stability in the $[A/B]_{4S}$ sequence compared to the $[A_4/B_4]_S$ sequence. For the min α_y optimization cases, GY70-Spectra/Epoxy, GY70-IM6/Epoxy, and GY70-AS4/Epoxy laminate designs yield the same results for both sequences. Moreover, the $[A/B]_{4S}$ sequence shows better dimensional stability performance in GY70-Kevlar 49/Epoxy and GY70-Aramid/Epoxy laminate designs, and the $[A_4/B_4]_S$ sequence provides a lower CTE-valued hybrid design with E-Glass/Epoxy.

In the results of AS4/Epoxy hybridized designs, it is noted for the min α_x optimization that the dimensional stability performance was obtained at the same level for AS4-E-Glass/Epoxy and AS4-

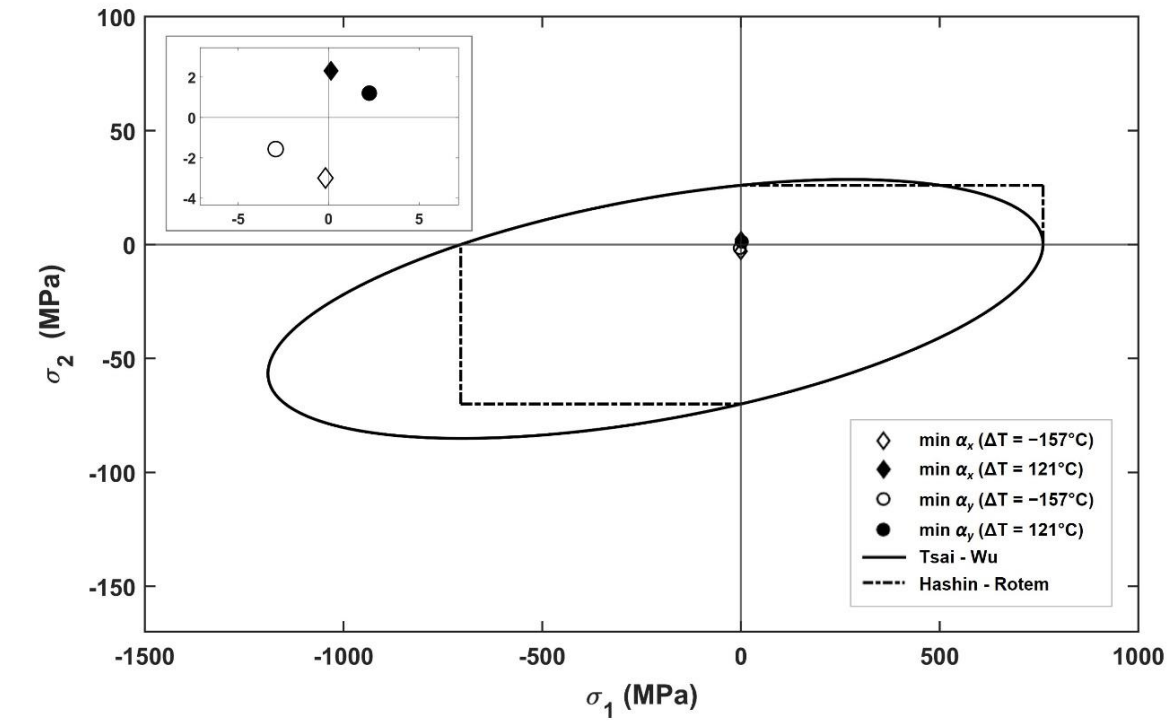
IM6/Epoxy hybrid laminates in both material sequences. Besides, lower CTE values for the $[A/B]_{4S}$ sequence were obtained in the hybrid designs of AS4-Kevlar 49/Epoxy and AS4-Aramid/Epoxy compared to the $[A_4/B_4]_S$ sequence results. However, it is seen that the AS4-Spectra/Epoxy hybrid gives a better min α_x result for the $[A_4/B_4]_S$ sequence than the $[A/B]_{4S}$ sequence. Regarding the min α_y optimization, lower CTE values were obtained at the same level for AS4-E-Glass/Epoxy, AS4-IM6/Epoxy, and AS4-GY70/Epoxy hybrid laminates in both material sequences. Similar to the min α_x case, lower CTE values for the $[A/B]_{4S}$ sequence were obtained in the hybrid designs of AS4-Kevlar 49/Epoxy and AS4-Aramid/Epoxy compared to the $[A_4/B_4]_S$ sequence results, whereas the AS4-Spectra/Epoxy hybrid gives better results for the $[A_4/B_4]_S$ sequence than the $[A/B]_{4S}$ sequence.

Considering the studies in the literature [9], [10], it can be seen that CTE values range between the orders of 10^{-6} and 10^{-7} in general. However, when compared to the results in the literature, minimum CTE values of up to the 10^{-10} order could be obtained by optimization, using continuous fiber angles in particular.

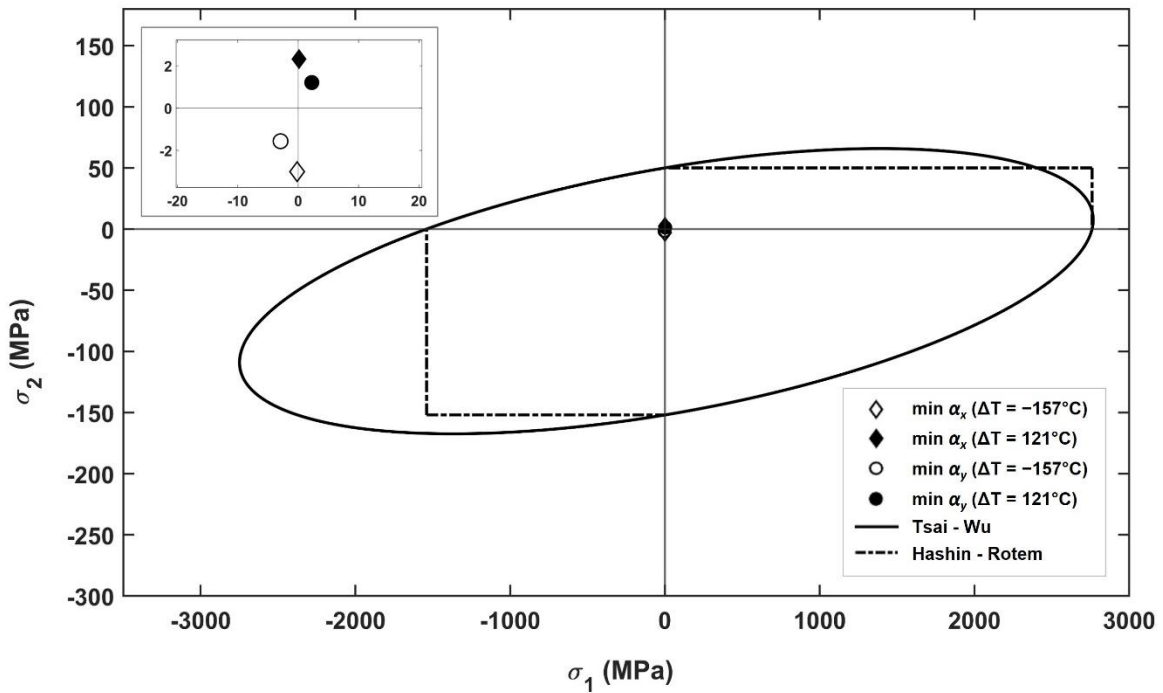
6.2. Dimensional Stability Performance of the Optimum Designs

In this section, the optimum hybrid min α_x and α_y designs that are better in terms of dimensional stability were selected to test their durability under specific thermal changes. Tsai-Wu and Hashin-Rotem failure criteria were considered to evaluate whether the hybrid composites in question would fail or not. Thermal loads were determined as a maximum negative and a maximum positive temperature change according to the reference values, $\Delta T = -157^\circ\text{C}$ and $\Delta T = 121^\circ\text{C}$, which were reported by NASA as the maximum temperature changes that materials in space are subjected to [28].

It is worth mentioning that the selection of the hybrid designs to be tested in terms of thermal durability was made according to the optimum designs with lower thermal expansion coefficient values among all designs. In this regard, for the $[A/B]_{4S}$ sequence, the selected optimum hybrid composites are GY70-IM6/Epoxy and AS4-E-Glass/Epoxy laminates of both traditional and continuous fiber-angled designs. Figures 4–7 show the thermal durability of these hybrid composites, respectively.

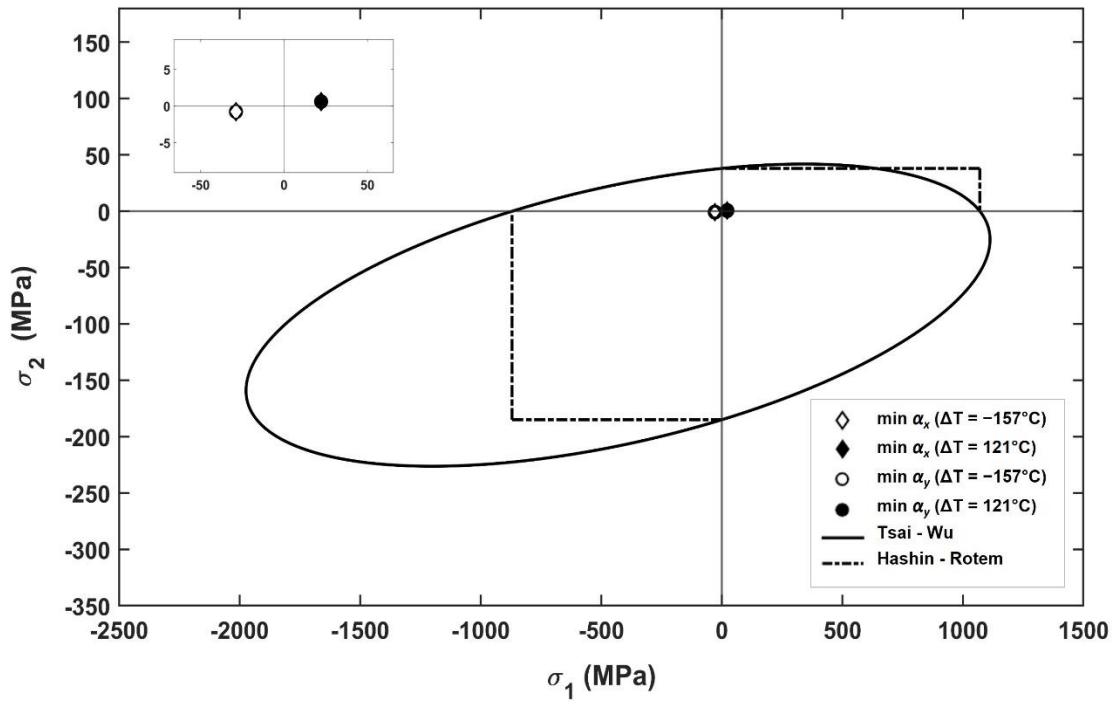


(a)

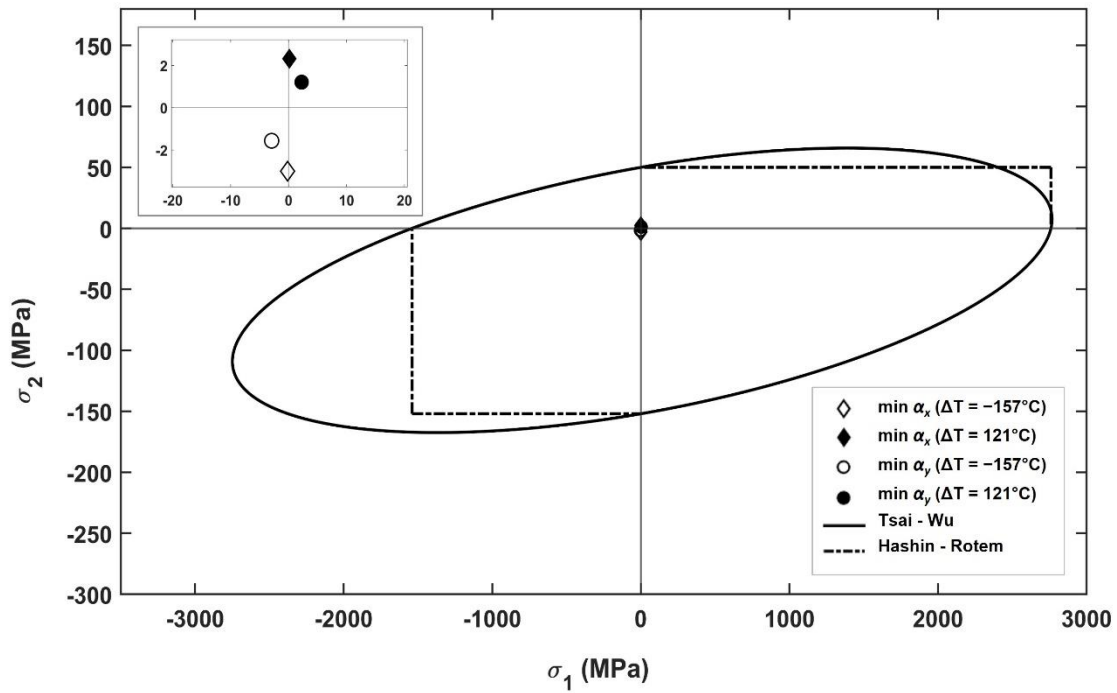


(b)

Figure 4. Thermal loading performances of $\min(\alpha_x)$ $[(0_{GY70}/90_{IM6})_3/45_{GY70}/90_{IM6}]_S$, and $\min(\alpha_y)$ $[(45_{GY70}/45_{IM6})_2/(90_{GY70}/90_{IM6})_2]$ hybrid designs: (a) GY70 laminate, (b) IM6 laminate

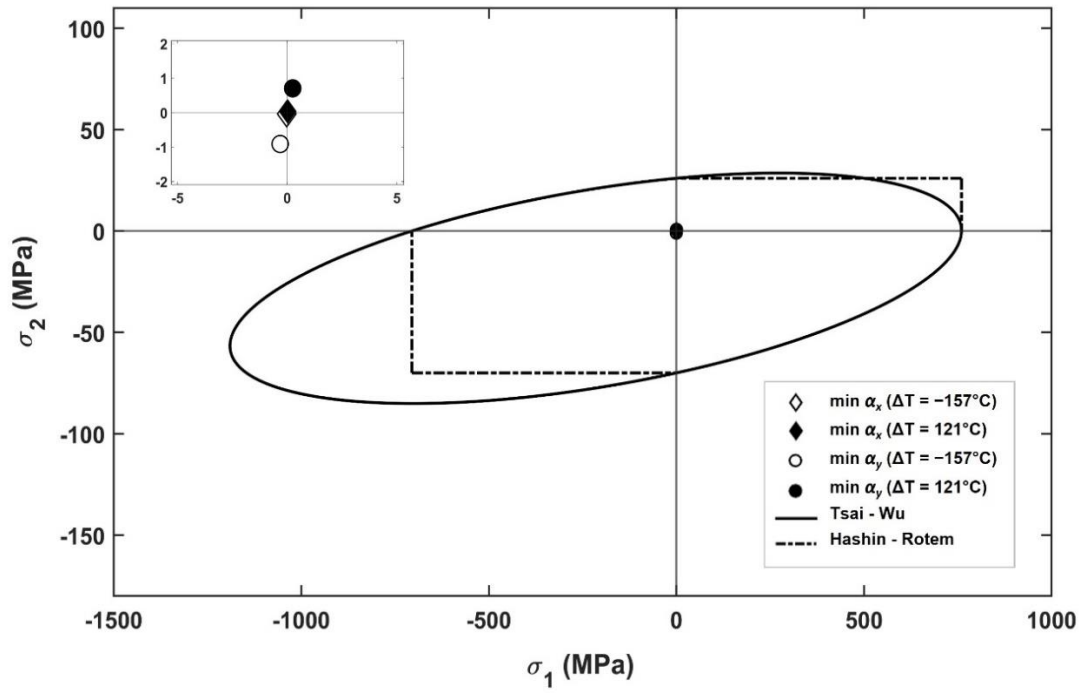


(a)

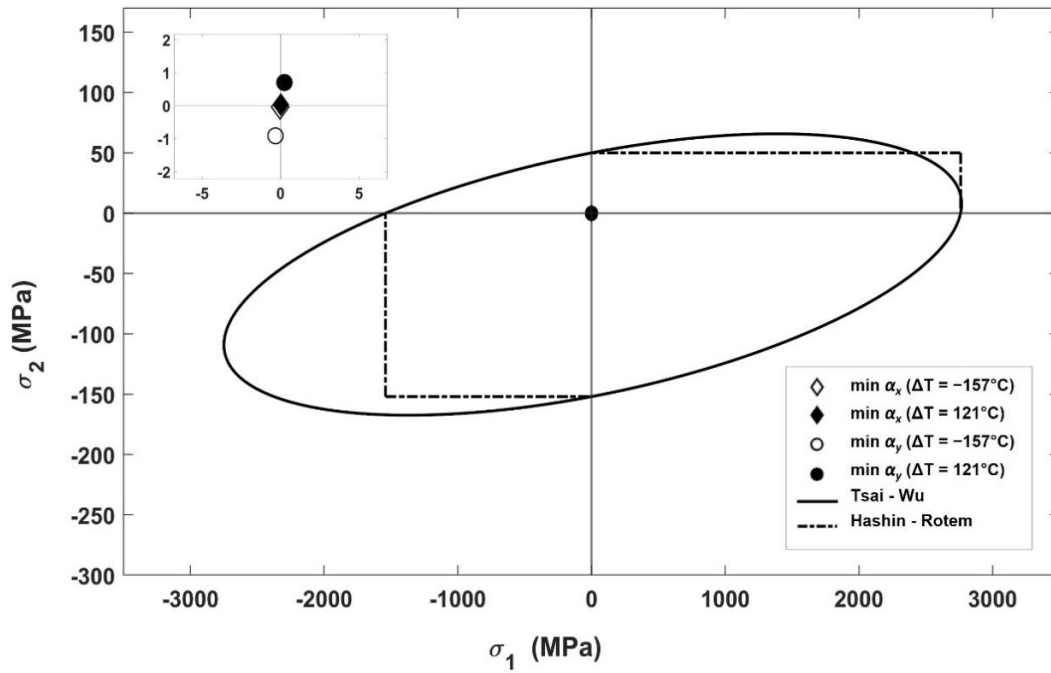


(b)

Figure 5. Thermal loading performances of $\min(\alpha_x)$ $[45_{AS4}/90_{Gl}]_{4S}$, and $\min(\alpha_y)$ $[45_{AS4}/0_{Gl}]_{4S}$ hybrid designs: (a) AS4 laminate, (b) E-Glass (Gl) laminate



(a)



(b)

Figure 6. Thermal loading performances of $\min(\alpha_x)$ $[41_{GY70}/8_{IM6}/52_{GY70}/23_{IM6}/51_{GY70}/8_{IM6}/27_{GY70}/26_{IM6}]_S$, and $\min(\alpha_y)$ $[90_{GY70}/35_{IM6}/35_{GY70}/7_{IM6}/64_{GY70}/39_{IM6}/42_{GY70}/44_{IM6}]_S$ hybrid designs: (a) GY70 laminate, (b) IM6 laminate

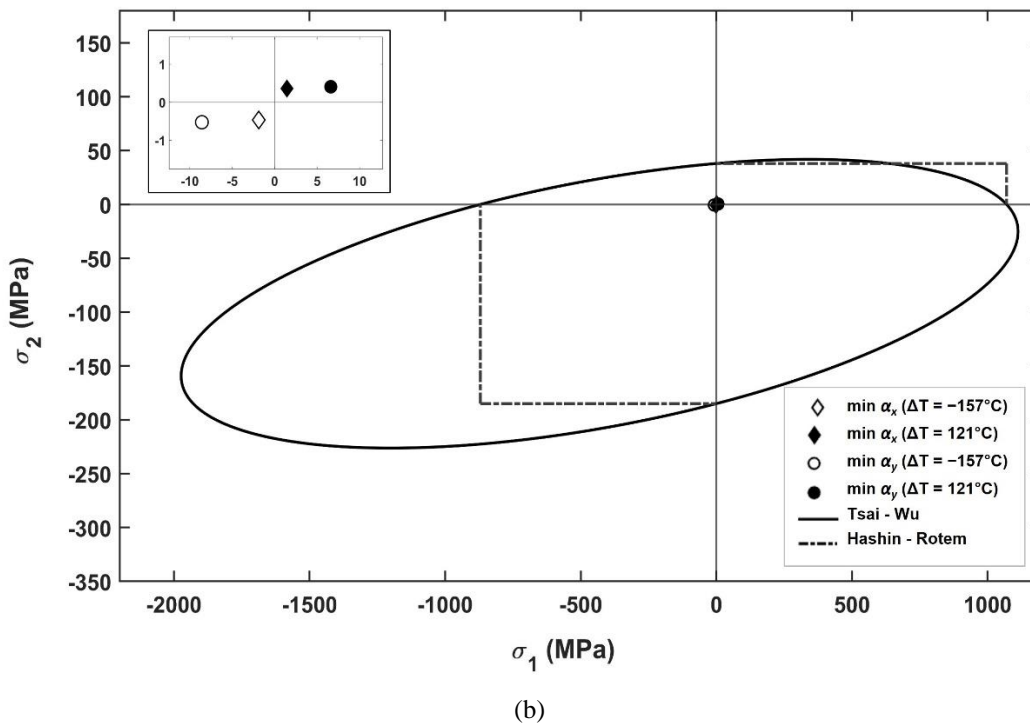
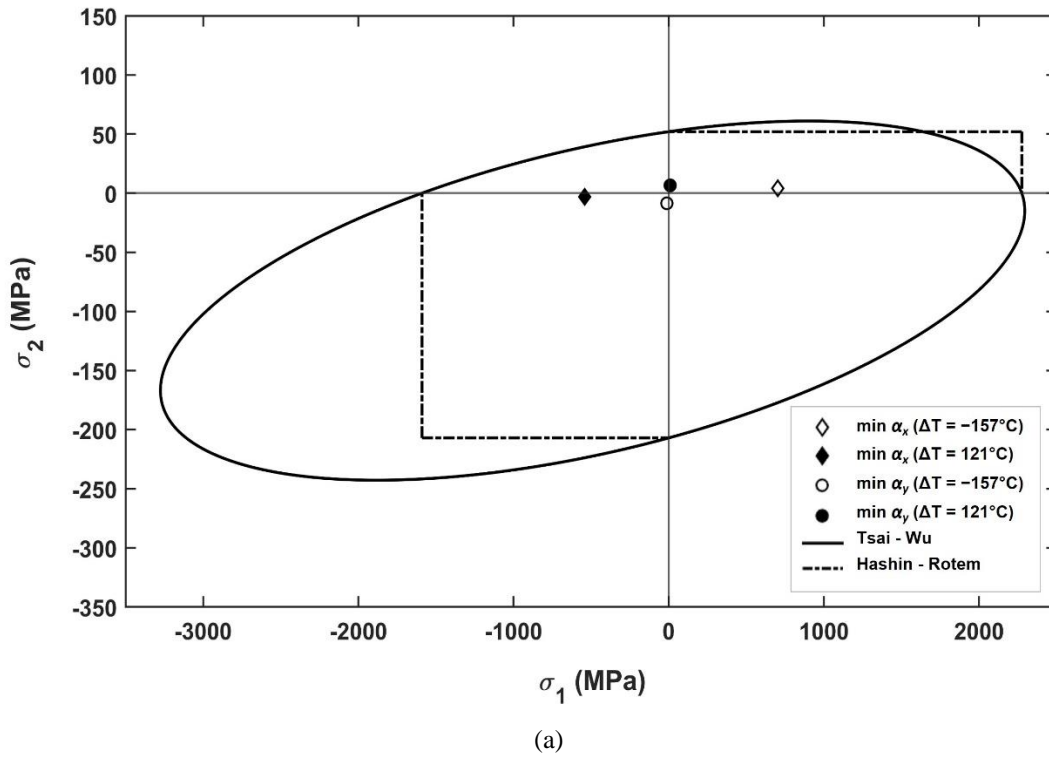
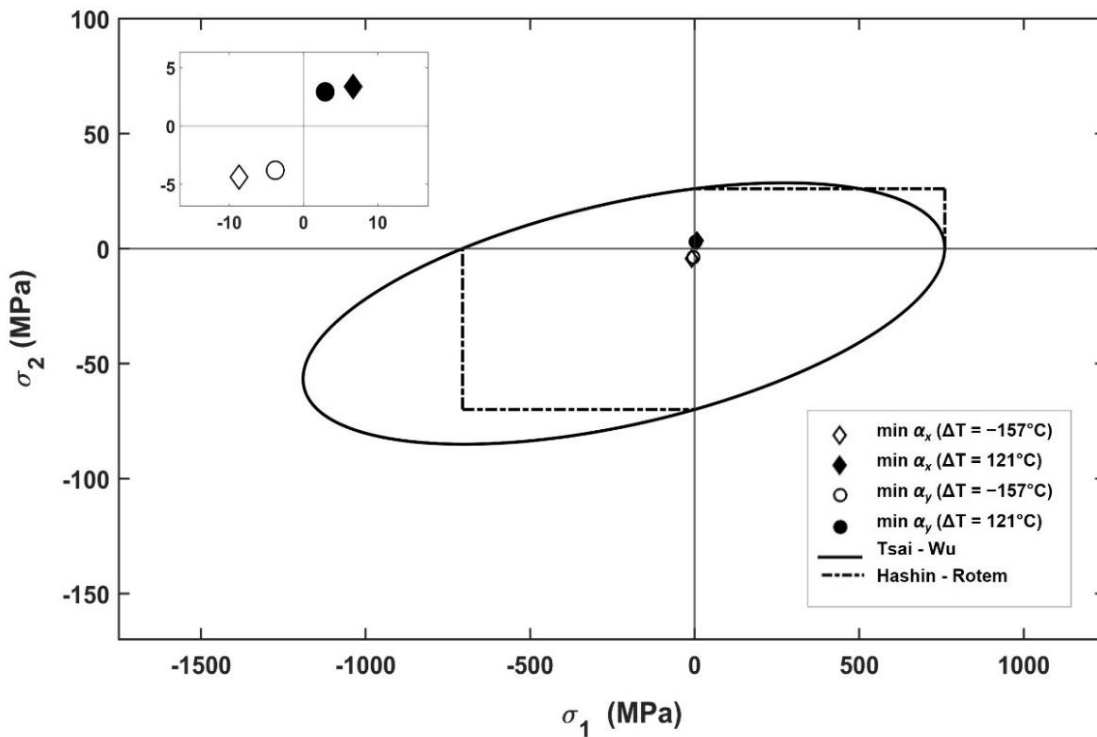


Figure 7. Thermal loading performances of $\min(\alpha_x)$ $[39_{AS4}/89_{GI}/42_{AS4}/83_{GI}/42_{AS4}/84_{GI}/39_{AS4}/83_{GI}]_s$, and $\min(\alpha_y)$ $[50_{AS4}/4_{GI}/53_{AS4}/4_{GI}/(50_{AS4}/4_{GI})_2]_s$ hybrid designs: (a) AS4 laminate, (b) E-Glass (GI) laminate

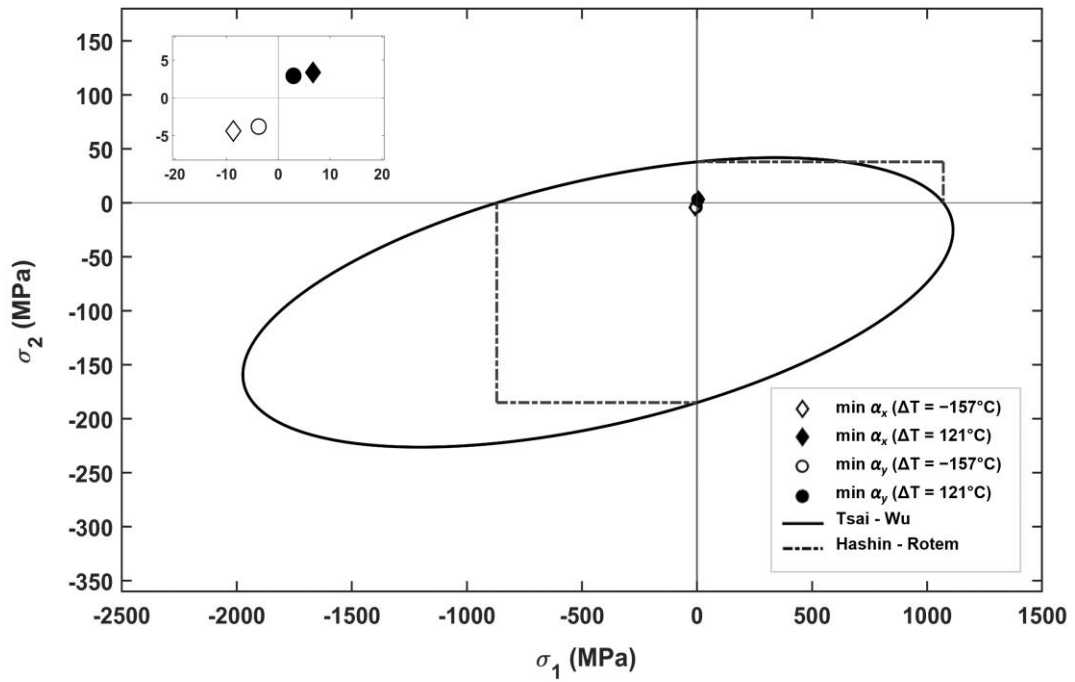
It is seen from the figures that $\min \alpha_x$ and $\min \alpha_y$ designs do not fail according to the Tsai-Wu (TW) and Hashin-Rotem (HR) failure criteria for all the layers, which is shown in detail in the small figure on the upper left of the figure. However, it can be noted that GY70/Epoxy and IM6/Epoxy laminates of $\min \alpha_x$ [(0_{GY70}/90_{IM6})₃/45_{GY70}/90_{IM6}]_s hybrid design (Figure 4) are very close to the failure limit under both thermal loads of $\Delta T = -157^\circ\text{C}$ and $\Delta T = 121^\circ\text{C}$ according to the Hashin-Rotem failure criterion. Considering Figure 5, it was observed that the AS4 laminates of $\min \alpha_x$ and $\min \alpha_y$ hybrid designs have the same failure index values, close to the failure limit of HR for each thermal load. Also, it can be said that E-Glass laminates of $\min \alpha_x$ design are on the critical edge of failure for both thermal loads. As for Figure 6, it is seen that thermal loads

cause relatively small values of stresses in the GY70 and IM6 laminates of the hybrid designs due to the utilization of continuous fiber angles in stacking sequences. A similar situation is also valid for the $\min \alpha_x$ and $\min \alpha_y$ designs of the AS4-E-Glass/Epoxy hybrid composite depicted in Figure 7.

As for the [A₄/B₄]_s sequence, the selected optimum hybrid designs are GY70-E-Glass/Epoxy laminates in both traditional and continuous designs. On the other hand, the selected optimum hybrid continuous designs of AS4/Epoxy include combinations with IM6/Epoxy and Spectra/Epoxy laminates. The thermal durability of these hybrid composites is shown in Figures 8–1, respectively.

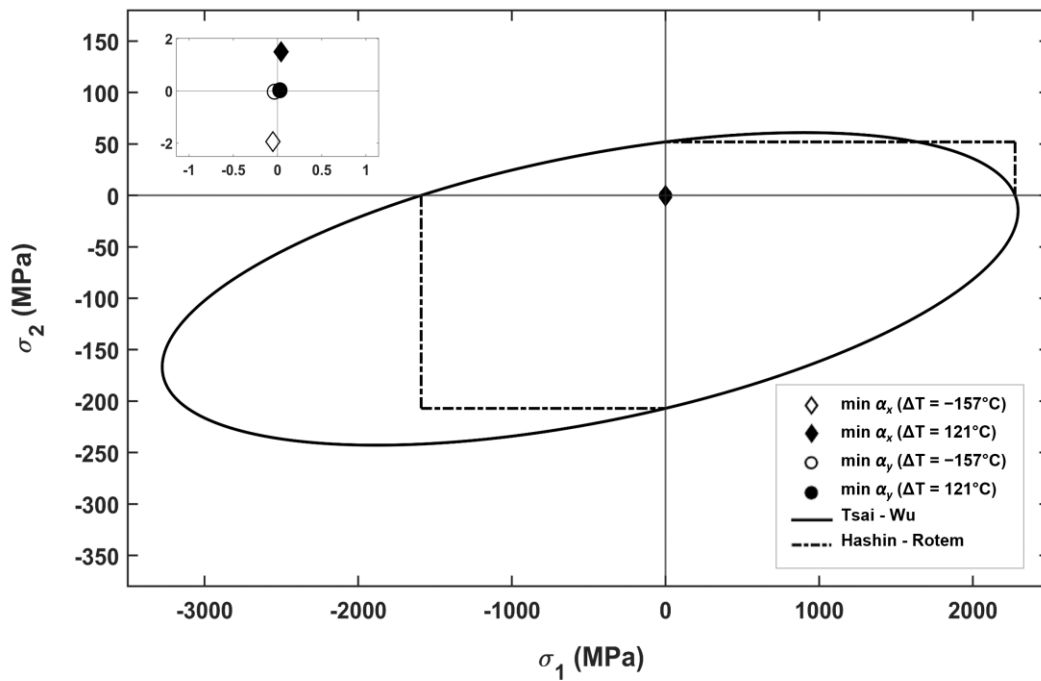


(a)

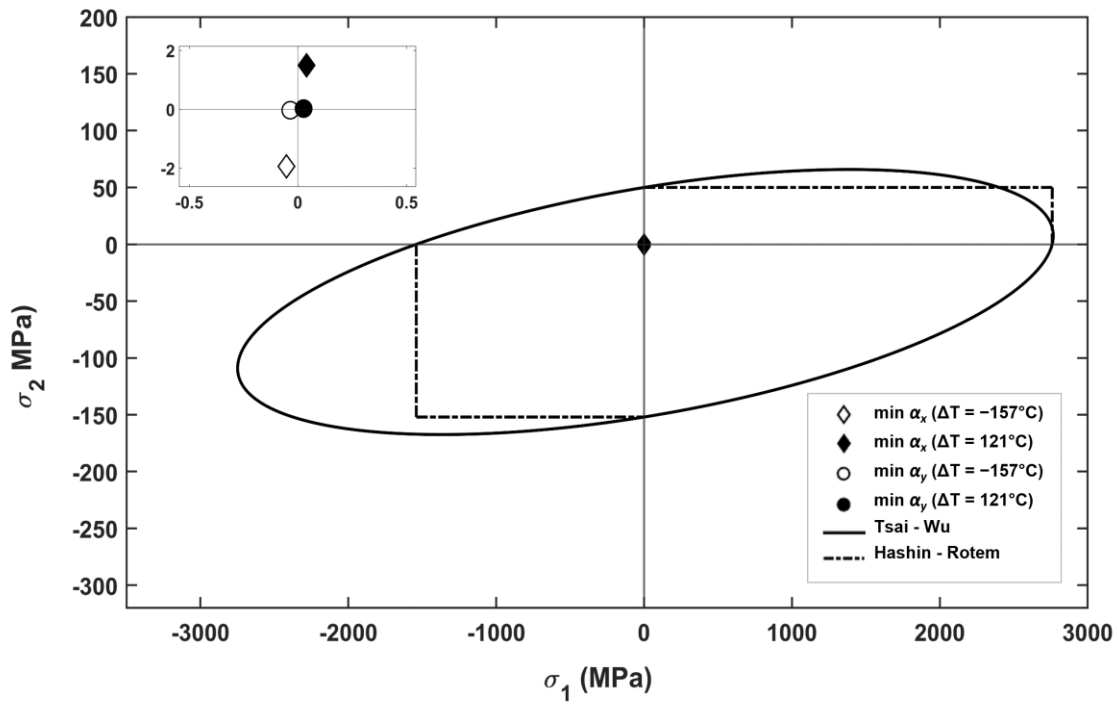


(b)

Figure 8. Thermal loading performances of $\min(\alpha_x)$ $[(90_{GY70})_2/(45_{GY70})_2/(45_{GI})_3/90_{GI}]_s$, and $\min(\alpha_y)$ $[(45_{GY70})_4/(45_{GI})_2/90_{GI}/45_{GI}]_s$ hybrid designs: (a) GY70 laminate, (b) E-Glass (GI) laminate

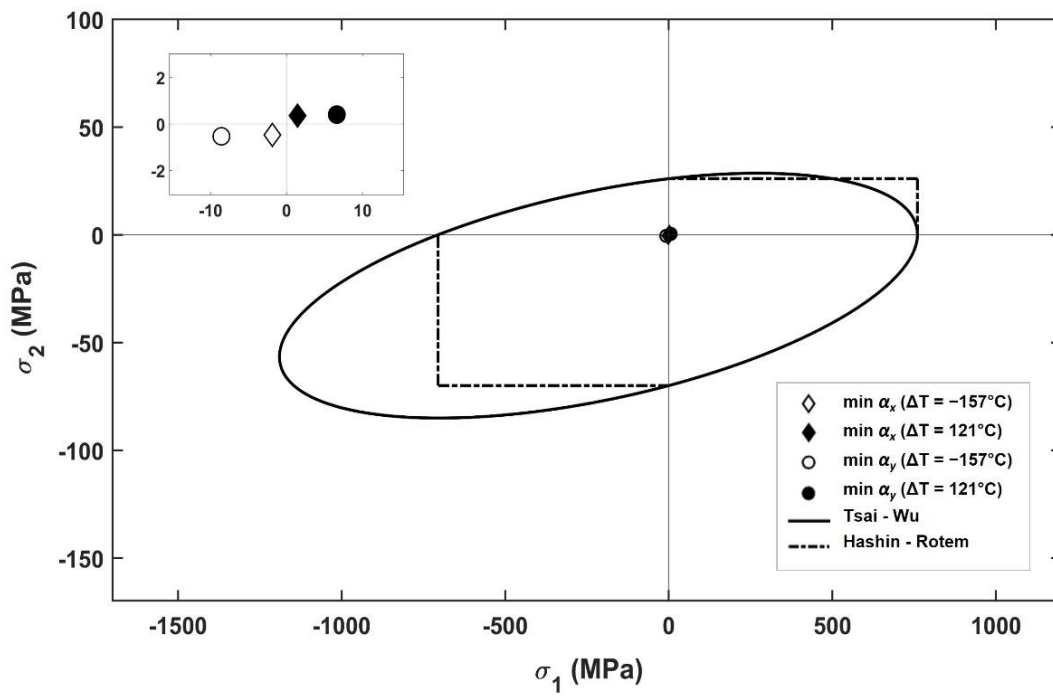


(a)

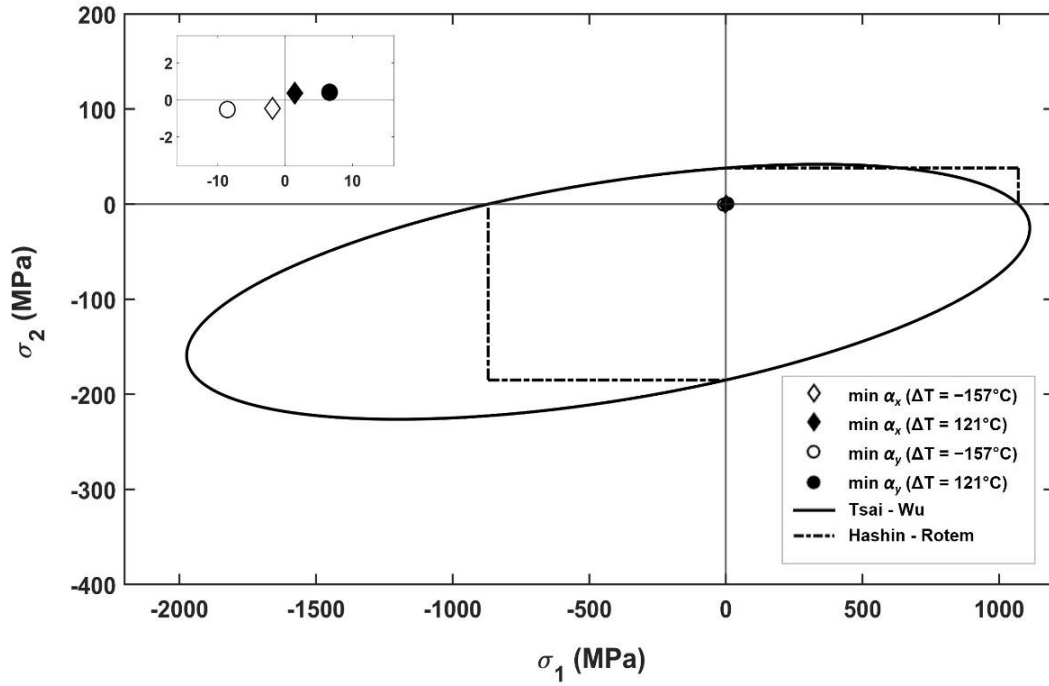


(b)

Figure 9. Thermal loading performances of $\min(\alpha_x)$ $[0_{AS4}/(45_{AS4})_3/90_{IM6}/(45_{IM6})_3]_S$, and $\min(\alpha_y)$ $[(90_{AS4})_4/(90_{IM6})_4]_S$ hybrid designs: (a)AS4 laminate, (b) IM6 laminate

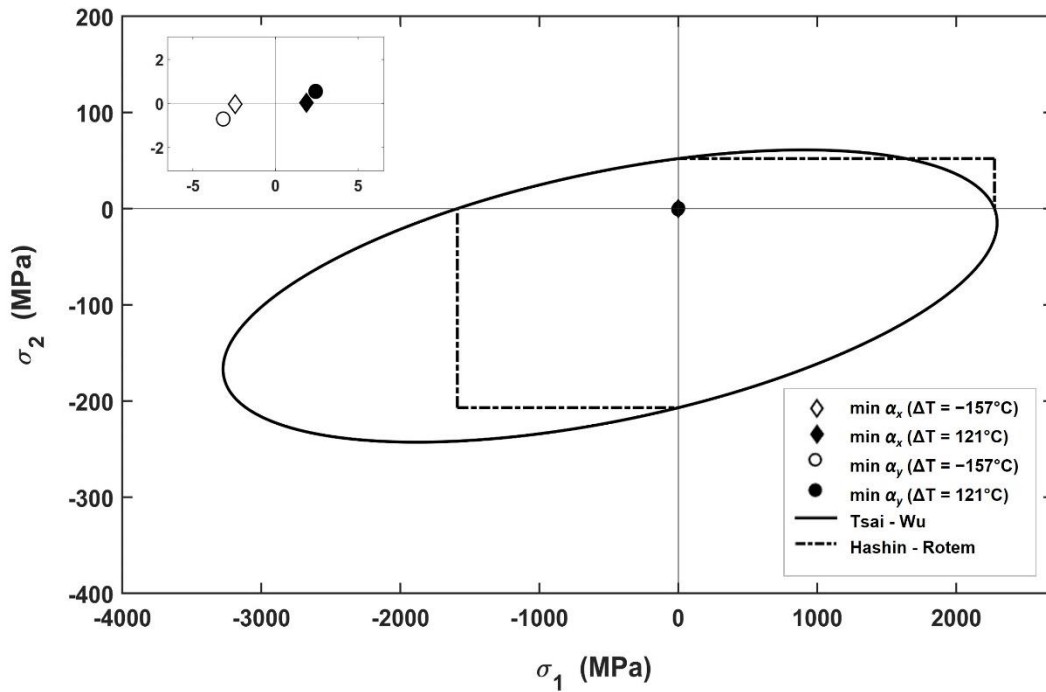


(a)



(b)

Figure 10. Thermal loading performances of min (α_x) [25_{AS4}/80_{AS4}/57_{AS4}/45_{AS4}/36_{IM6}/16_{IM6}/57_{IM6}/71_{IM6}]_s, and min (α_y) [0_{AS4}/84_{AS4}/89_{AS4}/36_{AS4}/49_{IM6}/46_{IM6}/48_{IM6}/5_{IM6}]_s hybrid designs: (a)AS4 laminate, (b) IM6 laminate



(a)

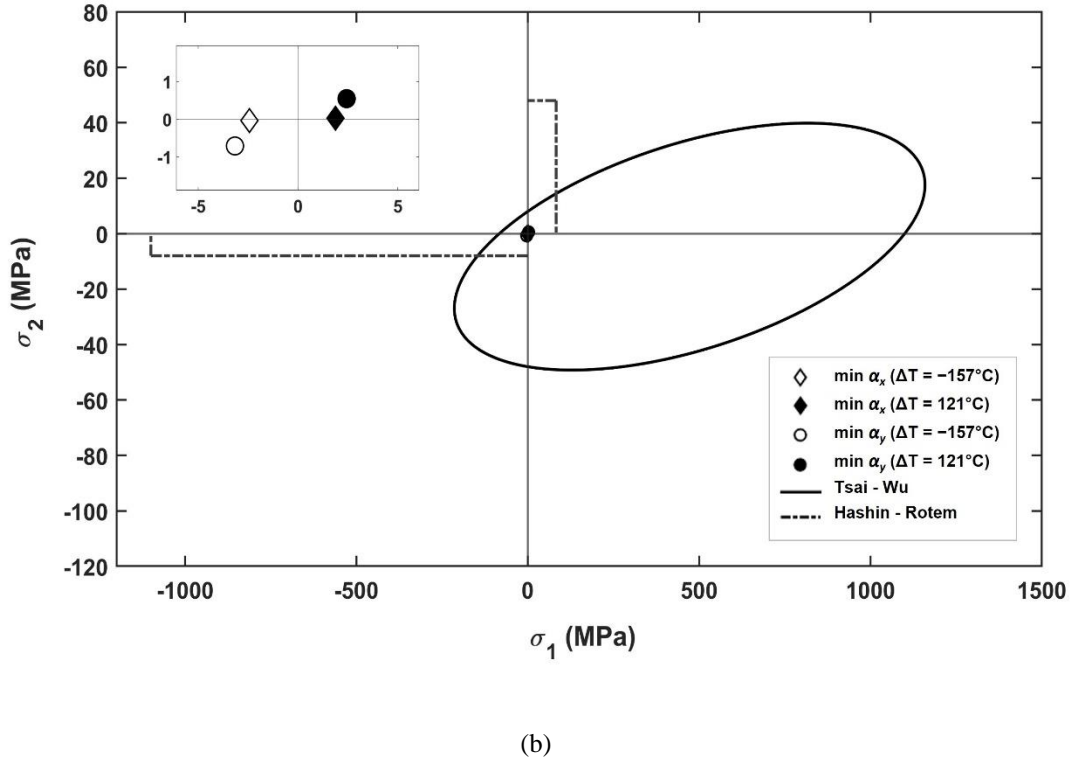


Figure 11. Thermal loading performances of min (α_x) $[61_{AS4}/56_{AS4}/(88_{AS4})_2/7_{Sp}/36_{Sp}/88_{Sp}/34_{Sp}]_S$, and min (α_y) $[1_{AS4}/28_{AS4}/(0_{AS4})_2/1_{Sp}/21_{Sp}/1_{Sp}/0_{Sp}]_S$ hybrid designs: (a)AS4 laminate, (b) IM6 laminate

Figures 8–11 show that min α_x and min α_y designs do not fail according to both Tsai-Wu (TW) and Hashin-Rotem (HR) failure criteria for all layers of the hybrid composites. That can be observed in more detail at the top left of all the figures. As in the case of the $[A/B]_{4S}$ sequence (Figures 4–7), it can be said that all the $[A_4/B_4]_S$ hybrid designs are readily within the safe zone according to the TW failure criterion. However, it seems that the stress values of many min α_x and min α_y designs are very close to the failure envelope of the HR failure criterion, even if these hybrid laminates can still be accepted in a safe zone. This situation can be noted mainly for the hybrid laminates presented in Figures 9 and 10.

7. Conclusion

In this study, the focus was on achieving dimensional stability optimization using hybrid composite materials. The selected hybrid composite materials to be used were Aramid/Epoxy, AS4/Epoxy, Boron/Epoxy, E-Glass/Epoxy, IM6/Epoxy, GY70/Epoxy, Kevlar49/Epoxy, and Spectra/Epoxy. The optimum fiber orientations in the $[A/B]_{4S}$ and

$[A_4/B_4]_S$ laminate sequences of the 16-layer hybrid composite laminates having minimum thermal expansion coefficients in the x and y directions were investigated by the GA/GPSA hybrid algorithm constituted via the MATLAB program.

All the non-hybrid and hybrid composite laminate results indicate that both optimum stacking sequences of the $[A/B]_{4S}$ and $[A_4/B_4]_S$ material sequences can minimize the thermal expansion coefficients, min α_x and min α_y up to the order of 10^{-10} . It was noted that $[A/B]_{4S}$ hybrid designs are slightly better than $[A_4/B_4]_S$ hybrid designs. When comparing the non-hybrid designs with all the hybrid designs, it was observed that the dimensional stability levels of the non-hybrid designs can be reduced to the order of 10^{-9} , whereas the hybrid designs can achieve even lower dimensional stability levels. Considering the continuous and traditional fiber-angled designs obtained through dimensional stability optimization, it was found that the optimum stacking sequences using continuous fiber angles provide better dimensional stability compared to the results of using traditional fiber angles in both material sequences. Furthermore, it can be stated that

all hybrid designs obtained for both material configurations exhibited dimensional stability levels according to the coefficients of thermal expansion ranging from 10^{-7} to 10^{-10} in general.

Additionally, the selected dimensionally stable hybrid designs were tested for their durability to temperature changes using the Tsai-Wu and Hashin-Rotem failure criteria. The results indicated that the majority of the selected optimum hybrid composite laminate designs were safe according to the failure criteria under positive and negative temperature changes. Overall, this study highlights the significant role of optimizing hybrid laminated composite laminate designs using various composite materials in achieving the maximum possible dimensional stability. Furthermore, these findings may provide valuable insights for future

optimization studies in the design of laminated composite materials, particularly for aerospace applications.

Contributions of the authors

The first author, Hacer Geçmez has run all the optimization problems defined earlier and wrote the paper. The second author, Hamza Arda Deveci has constituted the structure of the study, and supported the writing part.

Conflict of Interest Statement

There is no conflict of interest between the authors.

References

- [1] S. G. Lim and C. S. Hong, "Effect of transverse cracks on the thermomechanical properties of cross-ply laminated composites," *Compos. Sci. Technol.*, vol. 34, no. 2, pp. 145–162, 1989.
- [2] K. J. Yoon and J. Kim, "Prediction of Thermal Expansion Properties of Carbon/Epoxy Laminates for Temperature Variation," *J. Compos. Mater.*, vol. 34, no. 2, pp. 90–100, Jan. 2000.
- [3] R. Y. Kim and A. S. Crasto, "Dimensional stability of composites in space: CTE variations and their prediction," in *ICCM-10*, 1995, pp. 513–520.
- [4] R. L. Riche and R. Gaudin, "Design of dimensionally stable composites by evolutionary optimization," *Compos. Struct.*, vol. 41, no. 2, pp. 97–111, Feb. 1998.
- [5] M. Khalil, E. Bakhiet, and A. El-Zoghby, "Optimum design of laminated composites subjected to hygrothermal residual stresses," *Proc. Inst. Mech. Eng. L J. Mater. Des. Appl.*, vol. 215, no. 3, pp. 175–186, July 2001.
- [6] R. P. Zhu and C. T. Sun, "Effects of fiber orientation and elastic constants on coefficients of thermal expansion in laminates," *Mech. Adv. Mater. Struct.*, vol. 10, no. 2, pp. 99–107, 2003.
- [7] C. G. Diaconu and H. Sekine, "Flexural characteristics and layup optimization of laminated composite plates under hygrothermal conditions using lamination parameters," *J. Therm. Stresses*, vol. 26, no. 9, pp. 905–922, 2003.
- [8] L. Aydin and H. S. Artem, "Single and multi-objective genetic algorithm optimizations of the laminated composites used in satellite structures," in *Proceedings of the International Symposium of Mechanism and Machine Science*, Izmir, Turkey, 2010, pp. 219–226.
- [9] Z. Zhang, W. Zhong, and H. Song, "Design of hybrid composites with zero coefficient of thermal expansion," *J. Mater. Sci. Technol.*, vol. 12, no. 4, pp. 241–248, July 1996.
- [10] F. Bressan, F. De Bona, and A. Somà, "Design of composite laminates with low thermal expansion," *Proc. Inst. Mech. Eng. L J. Mater. Des. Appl.*, vol. 218, no. 3, pp. 201–209, July 2004.
- [11] S. Adali and K. Duffy, "Minimum cost design of vibrating laminates by hybridization," *Eng. Optim.*, vol. 19, no. 4, pp. 255–267, 1992.
- [12] S. Adali and V. E. Verijenko, "Optimum stacking sequence design of symmetric hybrid laminates undergoing free vibrations," *Compos. Struct.*, vol. 54, no. 2–3, pp. 131–138, Nov.-Dec. 2001.
- [13] M. Abachizadeh and M. Tahani, "An ant colony optimization approach to multi-objective optimal design of symmetric hybrid laminates for maximum fundamental frequency and minimum cost," *Struct. Multidiscipl. Optim.*, vol. 37, no. 4, pp. 367–376, Jan. 2009.
- [14] M. Savran and L. Aydin, "Stochastic optimization of graphite-flax/epoxy hybrid laminated composite for maximum fundamental frequency and minimum cost," *Eng. Struct.*, vol. 174, pp. 675–687, Nov. 2018.
- [15] A. K. Kaw, *Mechanics of composite materials*. Taylor and Francis, London, 2006.

- [16] H. A. Deveci, L. Aydın, and H. Seçil Artem, "Buckling optimization of composite laminates using a hybrid algorithm under Puck failure criterion constraint," *J. Reinf. Plast. Compos.*, vol. 35, no. 16, pp. 1233–1247, Aug. 2016.
- [17] S. W. Tsai and E. M. Wu, "A general theory of strength for anisotropic materials," *J. Compos. Mater.*, vol. 5, no. 1, pp. 58–80, Jan. 1971.
- [18] Z. Hashin and A. Rotem, "A fatigue failure criterion for fiber reinforced materials," *J. Compos. Mater.*, vol. 7, no. 4, pp. 448–464, Oct. 1973.
- [19] *MATLAB Optimization Toolbox. Computer software. Version R2019b*. The Mathworks, Inc. 2019.
- [20] T. Weise, "Global Optimization Algorithms Theory and Application," *Journal of Computer and Communications*, 2008.
- [21] X. S. Yang, *Engineering optimization: an introduction with metaheuristic applications*. NJ: John Wiley, 2010.
- [22] S. S. Rao, *Engineering optimization theory and practice*. NJ: John Wiley, 2009.
- [23] V. Torczon, "On the convergence of pattern search algorithms," *SIAM J. Optim.*, vol. 7, no. 1, pp. 1–25, 1997.
- [24] H. A. Deveci and H. S. Artem, "Optimum design of fatigue-resistant composite laminates using hybrid algorithm," *Compos. Struct.*, vol. 168, pp. 178–188, May 2017.
- [25] J. R. Vinson, R. L. Sierakowski, and C. W. Bert, "The behavior of structures composed of composite materials," *J. Appl. Mech.*, vol. 54, no. 1, pp. 249–249, 1987.
- [26] F. Donald, A. Leif, A. Carlsson, and R. Byron, *Experimental Characterization of Advanced Composite Materials*. New York, 2002.
- [27] R. R. Johnson, M. H. Kural, and G. B. Mackey, *Thermal Expansion Properties of Composite Materials*, California, 1981.
- [28] NASA, "Thermal loadings that materials in space can withstand," 2022. [Online]. Available: <https://www.nasa.gov/>. [Accessed: Dec.28, 2021].